

Can Entry-Wise Clipping Give Spectral Control of Stochastic Gradients?

Zitao Song* Cedar Site Bai* Zhe Zhang[†] Brian Bullins*
David F. Gleich*

Abstract

Training instabilities such as loss spikes are frequently the result of stochastic gradient noise. Because of rare expressions in language training data, and multiple layer composition, the noise impact is heavy-tailed and survives mini-batch averaging. Existing remedies trade off structure against cost: vector-norm clipping ignores the matrix structure of weight updates, while spectral normalization (e.g., Muon [1]) respects it at additional cost. We show that this trade-off can be balanced. Real gradient noise appears to be similar to entry-wise heavy-tailed contamination, and a first-order perturbation analysis reveals a *localization* property of such noise, under which a simple entry-wise method achieves spectral control. Exploiting this, we derive a tractable surrogate for the Bayes-optimal entry-wise estimator under a Gaussian signal prior. We establish $\mathcal{O}(\varepsilon^{-4})$ convergence guarantee under Cauchy-contaminated noise. Empirically, we find that smooth shrinkage improves Adam on NanoGPT pretraining, saving $\sim 7\%$ of training tokens. We further find that applying the entry-wise clipping before spectral normalization yields a $\sim 2\%$ token saving on top of Muon.

1 Introduction

A growing body of evidence shows that stochastic gradient noise is markedly heavy-tailed, with extreme entries occurring far more often than any Gaussian model would predict [2, 3]. In Large Language Model (LLM) pretraining [4, 5], these heavy tails are further amplified by model depth and scale, producing loss spikes and training instabilities [6, 7]. To address this, global [8] and coordinate-wise [9] gradient clipping truncate updates under vector-norm constraints, but neither controls the spectrum of matrix-valued weight updates.

Spectral methods [1, 10] offer a powerful alternative for constraining matrix-valued weight norms [11] and have shown success in LLM pretraining [12]. The Muon optimizer [1, 13] can be viewed as uniformly setting all singular values to one, and SPECTRA [14] generalizes this to spectral clipping under a random low-rank perturbation model, matching the performance of spectral normalization. However, spectral operations are computationally expensive, typically requiring SVD or Newton-Schulz iterations. This raises a natural question:

Can entry-wise clipping function as a cheap surrogate for spectral clipping in controlling the spectrum of matrix updates?

We show that the answer is yes under a heavy-tailed contamination model, but *not* under Gaussian or random low-rank noise with bounded second moment. The distinguishing property is *localization*: in real matrix-valued gradient noise, a small number of entries dominate the spectrum, whereas in Gaussian or random low-rank perturbations, no single entry can significantly perturb the spectrum. We formalize localization through the *normalized*

*Department of Computer Science, Purdue University, West Lafayette, IN, USA. Correspondence to: song903@purdue.edu, dgleich@purdue.edu

[†]School of Industrial Engineering, Purdue University, West Lafayette, IN, USA

localization ratio $\widehat{R}(E)$ of a noise matrix E , a metric derived from a first-order perturbation analysis of the top singular value. This metric identifies two regimes in which entry-wise magnitudes directly affect the perturbed spectrum, making entry-wise clipping a viable instrument for spectral control.

In particular, we observe that real stochastic noise from a transformer layer during large language model pretraining (Panels (a) and (e) in Figure 1) displays this localization phenomenon and resembles entry-wise heavy-tailed contamination (Panels (d) and (h)). Exploiting the entry-wise heavy-tailed structure, we derive *smooth shrinkage*, $\varphi(x) = xe^{-|x|/\tau}$, as a tractable surrogate for the Bayes-optimal entry-wise estimator that minimizes the first-order spectral perturbation under a Gaussian prior on the signal.

Contributions. Our contributions are threefold:

Localization metric and noise model. Through a first-order perturbation analysis of the top singular value (Theorem 3.3), we introduce the normalized localization ratio $\widehat{R}(E)$ (Definition 3.4) that quantifies how the largest entries of a noise matrix E align with the perturbation direction of the top singular value. We identify two regimes — $\widehat{R}(E) \gg 1$ and $\widehat{R}(E) \ll 1$ — in which entry-wise quantities can control the spectral perturbation. We verify that a heavy-tail contamination model (Definition 3.2), which reproduces the empirical heavy-tailed structure of gradient noise, falls into the $\widehat{R}(E) \gg 1$ localized regime.

Smooth shrinkage clipping. Under a Gaussian signal prior, we derive smooth shrinkage as a tractable surrogate for the Bayes-optimal entry-wise estimator that minimizes spectral perturbation in the localized regime (Theorem 4.1). Empirically, smooth shrinkage serves as an efficient substitute for spectral clipping: applied directly to the optimizer update (*post-clipping*, Section 2.2), it improves Adam by saving $\sim 7\%$ of training tokens; placed before spectral normalization (*pre-clipping*, Section 2.2), it also recovers subspace corrupted by localized spikes and improves Muon by saving $\sim 2\%$ of tokens.

Convergence theory. Under a known Cauchy-contaminated noise model, we establish convergence guarantees for stochastic gradient methods that apply either smooth shrinkage or hard coordinate-wise clipping at each of the two clipping stages: *post-clipping* and *pre-clipping*. In both cases, we prove an $\mathcal{O}(\varepsilon^{-4})$ complexity bound for finding an ε -stationary point, where the heavy-tail parameter enters only the complexity constants and not the exponent (Theorems 5.4 to 5.7).

Organization. Section 2 reviews preliminaries and related work on clipping methods. Section 3 introduces the entry-wise contamination model and analyzes its localization phenomenon. Section 4 exploits this localization to derive a new clipping operator, whose theoretical and empirical properties are established in Sections 5 and 6. Additional related work appears in Section A.

2 Preliminaries

Notation. For $A \in \mathbb{R}^{m \times n}$, $\sigma_i(A)$ denotes the i -th largest singular value with corresponding left/right singular vectors $u_i(A), v_i(A)$. We write $\|A\|_{\text{op}}, \|A\|_F, \|A\|_*$ for the spectral, Frobenius, and nuclear norms, $\|A\|_{\infty} := \max_{ij} |A_{ij}|$ for the entry-wise max, and $\langle A, B \rangle := \sum_{ij} A_{ij} B_{ij}$ for the Frobenius inner product. We write SVD as $A = U\Sigma V^T$ and $\text{msign}(A) := UV^T$.

2.1 Clipping Methods for Gradient Updates

For a matrix $G \in \mathbb{R}^{m \times n}$ and a threshold $c > 0$, we call a nonlinear map $\text{clip}_c(\cdot) : \mathbb{R}^{m \times n} \rightarrow \mathbb{R}^{m \times n}$ a *clipping map* if it controls the magnitude of gradient G below c under some norm. We briefly review three commonly used clipping maps.

Coordinate-wise clipping applies a scalar map independently to each entry of G :

$$\text{clip}_c^{\text{cw}}(G)_{ij} = \min(1, c/|G_{ij}|) G_{ij}. \quad (1)$$

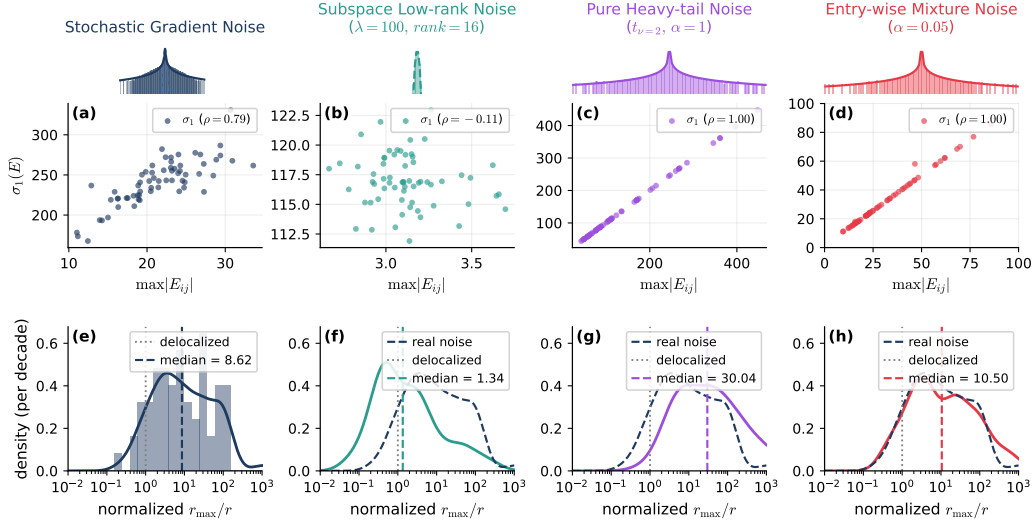


Figure 1: Entry-wise sparse heavy-tailed noise reproduces the spectral spikes observed in real stochastic gradients. The columns correspond to four noise models E , and the rows correspond to two diagnostics. *Real (a, e)*: minibatch gradient noise from a GPT-2 layer (`blocks.10.attn.qkv.w.v`). *Subspace low-rank (b, f)*: $E = \lambda \sum_{r=1}^K u_r v_r^T$ with $\lambda=100$, $K=16$, and u_r, v_r drawn uniformly from the unit sphere. *Pure heavy-tailed (c, g)*: entry-wise noise from Definition 3.2 with $\alpha=1$ and $H \sim t_2$. *Entry-wise mixture (d, h)*: entry-wise noise from Definition 3.2 with $\alpha=0.05$ and the same heavy-tailed component H as the previous column. All statistics are computed over 64 independent realizations. *Top strip*: marginal distribution of entries, normalized by each column’s empirical standard deviation. *Spectral-max scatter (a-d)*: $\max_{i,j} |E_{ij}|$ versus $\sigma_1(E)$, with Spearman ρ reported in each legend. A high ρ means the top singular value is driven by the largest entry. *Localization ratio (e-h)*: distribution of $\hat{R} = R/\text{median}[R_{\text{Gauss}}]$ from Definition 3.4; $\hat{R} \approx 1$ indicates E is indistinguishable from i.i.d. Gaussian noise, while $\hat{R} \gg 1$ indicates that a single entry of E carries a significant share of the leading-order spectral perturbation.

This guarantees $\|\text{clip}_c^{\text{cw}}(G)\|_\infty \leq c$, but absent additional structural assumptions on G , it offers no direct control over the spectral norm $\|\text{clip}_c^{\text{cw}}(G)\|_{\text{op}}$.

Global clipping [8] rescales the entire matrix whenever its Frobenius norm exceeds the threshold:

$$\text{clip}_c^{\text{g}}(G) = \min(1, c/\|G\|_F) G. \quad (2)$$

This ensures $\|\text{clip}_c^{\text{g}}(G)\|_F \leq c$, and hence $\|\text{clip}_c^{\text{g}}(G)\|_2 \leq c$, but it scales all entries uniformly, suppressing informative signal components together with noise.

Exact spectral clipping truncates each singular value at the threshold c given the SVD $G = U\Sigma V^T$:

$$\text{clip}_c^{\text{sp}}(G) = \sum_i \min(\sigma_i, c) u_i v_i^T. \quad (3)$$

This yields exact spectral-norm control, $\|\text{clip}_c^{\text{sp}}(G)\|_2 \leq c$, while preserving the singular-vector structure of G . However, computing the full SVD costs $O(mn \min(m, n))$. Recent work [14, 15] avoids an explicit SVD in spectral clipping via GPU-friendly *Newton-Schulz iterations* in BFloat16, but each iteration still incurs $O(mn \min(m, n))$ cost.

2.2 Stages for Gradient Clipping

Given iterates $X_k \in \mathbb{R}^{m \times n}$ and a clipping map $\text{clip}_c(\cdot)$ from Section 2.1, we categorize clipping methods in stochastic optimization into two groups based on the stage at which they are applied.

Post-clipping. We call $\text{clip}_c(\cdot)$ a *post-clipping* step when it is applied directly to a weight update U_k computed by a specific optimizer using stochastic gradient descent, yielding

$$X_{k+1} = X_k - \text{clip}_c(U_k). \quad (4)$$

When U_k is the stochastic gradient itself, this recovers Clipped SGD [9]; when U_k is the Adam update, it recovers Post-Spectral Clipping [14]. In the post-clipping regime, Clipped SGD and its variants are known to converge both in expectation [9] and with high probability [16, 17], even when the gradient variance is unbounded. Without post-clipping, standard SGD analyses break down in the heavy-tailed gradient noise regime [9].

Pre-clipping. We call $\text{clip}_c(\cdot)$ a *pre-clipping* step when it is applied before the spectral normalization step, popularized by Muon [1], yielding

$$X_{k+1} = X_k - \text{msign}(\text{clip}_c(M_k)), \quad (5)$$

where M_k can be a momentum buffer of the stochastic gradient \tilde{G} or the stochastic gradient itself. Originally, the pre-clipping map was introduced in [18] and [19] to stabilize the gradient accumulation before msign . While msign bounds the final update norm, the raw mini-batch average fed into msign can still be dominated by a single extreme heavy-tailed realization; as shown in Section 3 and Section 6, such outliers induce spectral spikes that corrupt and rotate the gradient matrix toward an outlier-driven subspace. Pre-clipping can mitigate this and help subspace identification by suppressing coordinate-induced spectral spikes prior to spectral normalization, yielding a signal-direction-preserving proxy for the true batch gradient.

3 Heavy-tailed Entries Can Drive Spectral Inflation

Let $G = \nabla f(X) \in \mathbb{R}^{m \times n}$ denote the true matrix gradient and $\tilde{G} = G + E$ denote the stochastic counterpart. In this section we compare two candidate models for the noise term E (Section 3.1) and ask under what conditions an entry-wise perturbation of G can meaningfully

alter its spectrum. Through a *localization* metric (Section 3.2), we show that a heavy-tailed mixture noise model induces spectral spikes whose effect on the top singular value can be controlled by entry-wise error minimization (Section 3.3). We empirically verify that real stochastic gradient noise exhibits the same heavy-tailed, localized structure (Figure 1).

3.1 Subspace Perturbation vs. Entry-wise Contamination

A recent work [14] models the gradient noise E as a rank- r subspace perturbation (Definition 3.1) with random orthonormal vectors U_r, V_r . Such a perturbation alters the spectrum of G by injecting a discrete cluster of spikes at the top of its singular value distribution.

Definition 3.1 (Subspace perturbation [20]). The noise is a rank- r matrix $E = \lambda U_r V_r^T$, where $\lambda > 0$ controls the spike magnitude and $U_r \in \mathbb{R}^{m \times r}$, $V_r \in \mathbb{R}^{n \times r}$ have orthonormal columns.

Under the bounded second-moment assumption $\mathbb{E}[U_r U_r^T] \leq cI_m$ [14], however, the Gaussian-like low-rank model is poorly aligned with the entry-wise heavy-tailed behavior of stochastic gradient noise: real gradients do not exhibit the exact Gaussian bulk structures that this model implies. As shown in the top strip of Figure 1, the entries of real gradients display heavy-tailed outliers that extend beyond the Gaussian bulk, a structure that low-rank perturbations with bounded second moment cannot reproduce. This motivates the entry-wise mixture model in Definition 3.2, which combines a heavy-tailed component with the Gaussian bulk to capture this effect.

Definition 3.2 (Entry-wise contamination). Each entry of E is drawn i.i.d. from Huber’s contamination model [21]:

$$E_{ij} \stackrel{\text{iid}}{\sim} (1 - \alpha) \mathcal{N}(0, \sigma^2) + \alpha H, \quad \alpha \in [0, 1], \quad (6)$$

where the contaminating distribution H is restricted to a symmetric heavy-tailed family (e.g., Cauchy(0, γ) or Student’s t_ν).

Heavy-tailed stochastic gradient noise has been studied by Simsekli, Sagun, and Gurbuzbalaban [2] and Zhang et al. [9]. In the large-scale language setting, it is further reinforced by the heavy-tailed nature of natural language itself, as captured by Zipf’s law [22, 23]. However, whether entry-wise noise of this form in the matrix updates can produce spectral spikes analogous to those of the subspace perturbation model remains unknown.

3.2 From First-order Perturbation to a Localization Metric

To understand when the entry-wise error inflates the spectrum, we first state a result based on first-order perturbation theory. (We were unable to find this specific result stated anywhere, but believe it to be fairly classical. It’s similar to results from Magnus [24] and Kato [25].)

Theorem 3.3 (First-order expansion of σ_1). *Let $G \in \mathbb{R}^{m \times n}$ have a simple top singular value $\sigma_1(G) > \sigma_2(G)$, with corresponding left and right singular vectors u_1 and v_1 , and let $\delta := \sigma_1(G) - \sigma_2(G)$ denote the spectral gap. There exists a universal constant $C > 0$ such that for every perturbation $E \in \mathbb{R}^{m \times n}$ with $\|E\|_{op} < \delta/4$,*

$$\sigma_1(G + E) = \sigma_1(G) + \sum_{ij} (u_1)_i (v_1)_j E_{ij} + \theta, \quad |\theta| \leq C \frac{\|E\|_{op}^2}{\delta}. \quad (7)$$

The above theorem shows that the leading-order change in σ_1 is a $(u_1)_i (v_1)_j$ -weighted sum of the entries of E , and it can further be extended to the rest of the singular values under the unique singular value assumption. A single heavily weighted entry of E can therefore dominate the perturbation. This motivates a metric, named as localization ratio, that quantifies how much of E ’s alignment with G ’s top singular direction is concentrated in a single entry rather than spread across the matrix.

Table 1: **Localization ratio (Definition 3.4) under three noise models.** The Gaussian noise has entries drawn i.i.d. from $\mathcal{N}(0, \sigma^2)$; the entry-wise spike noise has a single nonzero entry at location (i', j') ; the uv -aligned low-rank noise adopts the signal G 's top singular directions u, v as its rank-one component. Rates for the Gaussian column are stated up to constants in expectation, and the entry-wise spike and uv -aligned columns are deterministic.

	Gaussian Noise	Entry-wise Spike Noise	uv -Aligned Low-rank Noise
	$(E)_{ij} \stackrel{\text{iid}}{\sim} \mathcal{N}(0, \sigma^2)$	$E = e_{i'} e_{j'}^T$	$E = cuv^T$
$r_{\max}(E)$	$\Theta(\log(mn)/(mn)^2)$	$\Theta(1/(mn))$	$\Theta(1/(mn)^2)$
$r(E)$	$\Theta(1/(mn))$	$\Theta(1/(mn))$	$\Theta(1)$
$R(E)$	$\Theta(\log(mn)/(mn))$	$\Theta(1)$	$\Theta(1/(mn)^2)$
$\hat{R}(E)$	$\Theta(1)$	$\Theta(mn/\log(mn))$	$\Theta(1/mn \log(mn))$

Definition 3.4 (Localization ratio). Let $G, E \in \mathbb{R}^{m \times n}$, and $u \in \mathbb{R}^m, v \in \mathbb{R}^n$ be the top left and right singular directions of G . The *localization ratio* of E relative to G is

$$R(E) := \frac{r_{\max}(E)}{r(E)}, \quad r_{\max}(E) := \frac{\max_{i,j} |u_i E_{ij} v_j|^2}{\|E\|_F^2}, \quad r(E) := \frac{|\langle uv^T, E \rangle|^2}{\|E\|_F^2}. \quad (8)$$

The *normalized localization ratio* is obtained by rescaling $R(E)$ against a standard Gaussian baseline E_{Gauss} with i.i.d. entries:

$$\hat{R}(E) := R(E) / \text{median}[R(E_{\text{Gauss}})]. \quad (9)$$

Both r and r_{\max} measure how E projects onto uv^T as fractions of $\|E\|_F^2$: r is the full bilinear projection, while r_{\max} is its largest single-entry contribution. Their ratio $R(E)$ therefore captures the fraction of the projection concentrated in a single entry, and normalizing by the Gaussian baseline in $\hat{R}(E)$ rescales $R(E)$ to a Gaussian-relative scale where $\hat{R}(E_{\text{Gauss}}) = 1$. Under the delocalization assumption of $|u_i v_j| = \Theta(1/\sqrt{mn})$, the behavior of these quantities under three representative noise models is summarized in Table 1.

The table makes $\hat{R}(E)$ usable as a directional-structure test on E . When $\hat{R}(E) \ll 1$, E 's projection onto uv^T is more significant than the Gaussian baseline, indicating a coherent low-rank component aligned with G 's top singular direction. When $\hat{R}(E) \gg 1$, a single entry contributes a critical share of the projection, indicating spike-like contamination. When $\hat{R}(E) \approx 1$, E is indistinguishable from isotropic Gaussian noise. We call E *localized* in either of the first two cases ($\hat{R}(E) \ll 1$ or $\hat{R}(E) \gg 1$) and *delocalized* in the third ($\hat{R}(E) \approx 1$).

3.3 From Localization to Entry-wise Minimization

We now show how the localization metric can be leveraged to control the top singular value of the noisy signal through minimizing the entry-wise error. The proposition below characterizes such optimal entry-wise estimator under an i.i.d. Gaussian prior on the clean signal G .

Proposition 3.5 (First-order spectral control via entrywise MSE). *Let $\tilde{G}_{ij} = G_{ij} + E_{ij}$, and $\Delta := \varphi(\tilde{G}) - G$ for an arbitrary entrywise estimator φ . When spectral gap $\delta > 4\|\Delta\|_{\text{op}}$, replacing $E \rightarrow \Delta$ in Theorem 3.3 and applying Cauchy-Schwarz to the leading term yields*

$$\mathbb{E}[\|\sigma_1(\varphi(\tilde{G})) - \sigma_1(G)\|^2] \leq \sum_{i,j} \mathbb{E}[(\varphi(\tilde{G}_{ij}) - G_{ij})^2] + o(\|\Delta\|_{\text{op}}^2/\delta). \quad (10)$$

If we place an entrywise prior to signal G , i.e., $G_{ij} \stackrel{\text{iid}}{\sim} \mathcal{N}(0, \sigma_x^2)$, the leading right-hand side is minimized coordinate-wise by $\varphi^*(y) = \mathbb{E}[x | y]$, where (x, y) denotes the entry pair (G_{ij}, \tilde{G}_{ij}) .

Remark 3.6. The bound in Proposition 3.5 is approximately saturated when $\hat{R}(\Delta) \ll 1$ (Δ concentrates along $u_1 v_1^T$), so entry-wise MSE minimization is essentially equivalent to minimizing the top singular-value perturbation. When $\hat{R}(\Delta) \gg 1$, the bound is loose, but the dominant spike entries of Δ are themselves sparse, and entry-wise minimization suppresses them directly. When $\hat{R}(\Delta) \approx 1$, Δ is delocalized and entry-wise minimization cannot selectively control the spectrum.

Following Remark 3.6, the spectral perturbation admits entry-wise control in either of the two localized regimes identified there, $\hat{R}(\Delta) \ll 1$ and $\hat{R}(\Delta) \gg 1$. In both cases the Bayes-optimal MMSE estimator $\mathbb{E}[G_{ij} | \tilde{G}_{ij}]$ is first-order optimal. The latter regime is the more attractive of the two: the underlying entry-wise spike noise can be modeled directly by a sparse heavy-tailed contamination without extra knowledge of the signal's true singular directions.

4 Smooth Shrinkage: A Bayes-Motivated Entry-Wise Spectrum Control

Here we focus on the $\hat{R}(\Delta) \gg 1$ regime, in which localization is induced by the entry-wise contamination model of Definition 3.2. Our main result identifies a closed-form surrogate for the Bayes-optimal entry-wise estimator in Proposition 3.5 that is asymptotically faithful in the large- $|\tilde{G}_{ij}|$ region, where heavy-tailed contamination dominates.

Theorem 4.1 (Smooth shrinkage as a Bayes-motivated surrogate). *Let $y = x + e$, where $x \sim \mathcal{N}(0, \sigma_x^2)$ and $e \sim (1 - \alpha)\mathcal{N}(0, \sigma^2) + \alpha H$ with $\alpha \in [0, 1)$, and the heavy tailed density h associated with H satisfies the score and curvature conditions of Lemma D.3. Define the Wiener coefficient $\beta := \sigma_x^2 / (\sigma_x^2 + \sigma^2)$ and the (Bayesian) retention probability $\pi(y) := \Pr(e \sim \mathcal{N} | y)$.*

- (i) **Asymptotic Bayes structure.** *For every $\varepsilon > 0$ there exists an explicit threshold $y^* = y^*(\varepsilon, h, \sigma_x) \in (0, \infty)$ such that for all $|y| \geq y^*$ the Bayes optimal entrywise estimator admits the factorization*

$$\mathbb{E}[x | y] = \pi(y) \beta y + \rho(y), \quad |\rho(y)| \leq \varepsilon. \quad (11)$$

Combined with the entrywise MSE upper bound of Proposition 3.5, this controls the spectral perturbation $\mathbb{E}[\sigma_1(\varphi_\tau(\tilde{G})) - \sigma_1(G)]^2$.

- (ii) **Unique closed form surrogate.** *Among continuous functions $\hat{\pi} : [0, \infty) \rightarrow (0, 1]$ satisfying $\hat{\pi}(y) \rightarrow 0$ as $y \rightarrow \infty$ (redescending), $\hat{\pi}(y_1 + y_2) = \hat{\pi}(y_1) \hat{\pi}(y_2)$ (multiplicative), and $\hat{\pi}(0) = 1$ (unit at origin), the unique one parameter family is $\hat{\pi}(y) = e^{-y/\tau}$ for some $\tau > 0$. Replacing π in Equation (11) with the even extension $y \mapsto e^{-|y|/\tau}$ yields the smooth shrinkage operator*

$$\varphi_\tau(y) := \beta e^{-|y|/\tau} y. \quad (12)$$

By Theorem 4.1, smooth shrinkage damps each entry y by a factor of $e^{-|y|/\tau}$, whereas hard coordinate-wise clipping (Equation (1)) applies a damping factor of $\min\{1, c/|y|\}$. Setting $c = \tau/e$ aligns the two damping curves: they are tangent at $|y| = \tau$, where both equal $1/e$. For $|y| > \tau$, however, smooth shrinkage's exponential decay imposes a strictly stronger penalty than hard clipping's $1/|y|$ tail. Figure 2 and Figure 5 illustrate this difference.

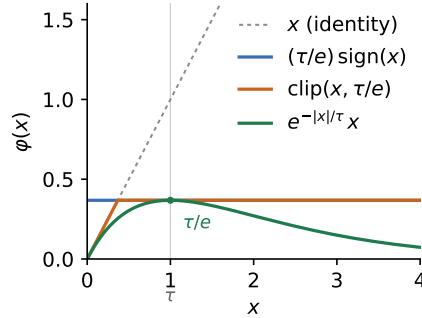


Figure 2: Three entry-wise operators on $x \geq 0$ with $\tau = 1$. We set $\beta = 1$ for smooth shrinkage in Equation (12).

Proof sketch of Theorem 4.1. (i) We first introduce a latent indicator $Z \in \{\mathcal{N}, H\}$ for the noise type generating y . By the tower property, $\mathbb{E}[x | y]$ is divided into $\mathbb{E}[x | y, Z = \mathcal{N}]$ and $\mathbb{E}[x | y, Z = H]$ two branches. The Gaussian branch is conjugate and exact: $\mathbb{E}[x | y, Z = \mathcal{N}] = \beta y$. The heavy-tailed branch has no closed form, but Lemma D.3 shows that for $|y| \geq y^*$ the heavy-tailed likelihood overwhelms the Gaussian prior, so the posterior collapses to the prior mean $\mathbb{E}[x] = 0$ up to error ε . Combining the two branches yields Equation (11). (ii) For $y \geq 0$, Bayes' rule together with the heavy-tail dominance from (i) gives $\hat{\pi}(y) \rightarrow 0$ as $y \rightarrow \infty$. Independence of the additive noise components implies the multiplicative identity $\hat{\pi}(y_1 + y_2) = \hat{\pi}(y_1) \hat{\pi}(y_2)$, which is Cauchy's exponential functional equation. Under continuity and $\hat{\pi}(0) = 1$, its only solutions are $\hat{\pi}(y) = e^{-y/\tau}$ for some $\tau > 0$. Even-extending to \mathbb{R} and substituting into Equation (11) produces the smooth shrinkage operator $\varphi_\tau(y) = \beta e^{-|y|/\tau} y$. The completed proof is provided in Section D. \square

5 Convergence Analysis

Consider a matrix-valued objective function $f : \mathbb{R}^{m \times n} \rightarrow \mathbb{R}$ with true gradient $G = \nabla f(X) \in \mathbb{R}^{m \times n}$. We evaluate the convergence result of the hard clipping map $C_\tau(x)$ and the newly introduced smooth shrinkage map $S_c(x)$ as two distinct entry-wise clipping methods at both *post-clipping* and *pre-clipping* stages. The definitions of $C_\tau(x)$ and $S_c(x)$ follow:

$$C_\tau(x) := x \min\{1, \tau/|x|\}, \quad S_c(x) := x e^{-|x|/c}, \quad (13)$$

where we use the threshold c for smooth shrinkage in this section to distinguish it from τ used by the hard clipper. We drop the Wiener coefficient β in equation 12 since it can be absorbed into the learning rate. Under a known entry-wise contamination model, we establish the standard $\mathcal{O}(\varepsilon^{-4})$ sample complexity result for reaching the first-order stationarity of a nonconvex function. The overall complexity using two different clipping methods is summarized in Table 2.

Assumption 5.1 (Smoothness). For $X, Y \in \mathbb{R}^{m \times n}$, the objective $f : \mathbb{R}^{m \times n} \rightarrow \mathbb{R}$ is L -smooth in the Frobenius norm: $f(Y) \leq f(X) + \langle \nabla f(X), Y - X \rangle + \frac{L}{2} \|Y - X\|_F^2$. Moreover, we assume the objective is bounded below such that $\Delta := f(X_0) - \inf_X f(X) < \infty$. We denote $G_k := \nabla f(X_k)$ and let $d := mn$.

Assumption 5.2 (Bounded True Gradients). There exists a constant $B < \infty$ such that the ℓ_∞ norm of the true gradient is bounded for all iterates: $\|G_k\|_\infty = \max_{i,j} |(G_k)_{i,j}| \leq B$.

Assumption 5.3 (Entry-wise Noise Model). Given X_k , a noisy gradient sample takes the form $G_k + \Xi_k$. Ξ_k is independent of X_k and across iterates k . Each entry ξ_k in Ξ_k follows a symmetric noise mixture model: $\xi_k \sim (1 - \alpha)\mathcal{N}(0, \sigma_k^2) + \alpha \text{Cauchy}(0, \gamma_k)$, where $0 \leq \alpha \leq 1$, $\sigma_k \geq 0$, and $\gamma_k > 0$. For all iterates, the local scales are uniformly bounded by $\sigma, \gamma > 0$ such that $\sigma_k \leq \sigma$ and $\gamma_k \leq \gamma$.

5.1 Convergence Result for Post-clipping

Given an entry-wise mapping $\varphi : \mathbb{R}^{m \times n} \rightarrow \mathbb{R}^{m \times n}$, we consider the following single-sample clipped stochastic gradient update:

$$X_{k+1} = X_k - \eta \varphi(G_k + \Xi_k), \quad (14)$$

The subsequent theorems establish the convergence guarantees when the mapping φ is instantiated as either the hard-clipping function C_τ or the smooth-shrinkage function S_c .

Table 2: **Main convergence results for *post-clipping* and *pre-clipping*.** S_c and C_τ are two different clipping methods with threshold c and τ introduced in Equation (13). The complexity column counts iterations K (post-clipping) or T (pre-clipping); pre-clipping additionally uses N samples per iteration, so its total sample budget is $TN = \mathcal{O}(L\Delta D^2 r^4 v_\bullet \varepsilon^{-4})$ whereas post-clipping requires $\mathcal{O}(L\Delta d c_\bullet^2 \varepsilon^{-4})$ with $\bullet \in \{\tau, c\}$. Explicit constants are presented in Theorems 5.4 to 5.7.

Method	Clipping Threshold scale	Stationarity	Complexity
Post (C_τ)	$\tau \gtrsim B + \sigma + \alpha\gamma$	$\sum \mathbb{E}\ G_k\ _F/K \leq \varepsilon$	$\mathcal{O}(L\Delta d\tau^2 \varepsilon^{-4})$
Post (S_c)	$c \gtrsim B + (1 - \alpha)\sigma + \alpha\gamma \log(e + \alpha)$	$\sum \mathbb{E}\ G_k\ _F/K \leq \varepsilon$	$\mathcal{O}(L\Delta d c^2 \varepsilon^{-4})$
Pre (C_τ)	$\tau \gtrsim B + \sigma\sqrt{\log r} + \alpha\gamma\sqrt{r}$	$\sum \mathbb{E}\ G_k\ _*/T \leq \varepsilon$	$\mathcal{O}(L\Delta D^2 r^4 v_\tau \varepsilon^{-4})$
Pre (S_c)	$c \gtrsim \sqrt{r}\{B + (1 - \alpha)\sigma + \alpha\gamma \log(e + \alpha\sqrt{r})\}$	$\sum \mathbb{E}\ G_k\ _*/T \leq \varepsilon$	$\mathcal{O}(L\Delta D^2 r^4 v_c \varepsilon^{-4})$

Theorem 5.4 (Post-clipping with hard clipping). *Under Assumptions 5.1 to 5.3, choose τ such that $\tau \geq B + \max\{\sigma\sqrt{2\log 8}, \frac{8\alpha\gamma}{\pi}\}$. Executing the update rule Equation (14) with $\varphi = C_\tau$ and a step size of $\eta = \sqrt{2\Delta/(L\tau^2 dK)}$ for K iterations yields:*

$$\frac{1}{K} \sum_{k=0}^{K-1} \mathbb{E}\|G_k\|_F^2 \leq 2\tau \sqrt{\frac{2L\Delta d}{K}}. \quad (15)$$

Consequently, when $K \geq 8L\Delta d\tau^2/\varepsilon^4$, we guarantee $\frac{1}{K} \sum_{k=0}^{K-1} \mathbb{E}\|G_k\|_F \leq \varepsilon$.

Theorem 5.5 (Post-clipping with smooth shrinkage). *Under Assumptions 5.1 to 5.3, choose $c \geq \max\left\{4\left[B + \sqrt{\frac{8}{\pi}}(1 - \alpha)\sigma\right], \frac{64\alpha\gamma}{\pi} \log\left(e + \frac{64\alpha}{\pi}\right)\right\}$. Executing the update rule Equation (14) with $\varphi = S_c$ and a step size of $\eta = e\sqrt{2\Delta/(Lc^2 dK)}$ for K iterations yields:*

$$\frac{1}{K} \sum_{k=0}^{K-1} \mathbb{E}\|G_k\|_F^2 \leq \frac{2c}{e} \sqrt{\frac{2L\Delta d}{K}}. \quad (16)$$

Consequently, when $K \geq 8L\Delta d c^2/(e^2 \varepsilon^4)$, we guarantee $\frac{1}{K} \sum_{k=0}^{K-1} \mathbb{E}\|G_k\|_F \leq \varepsilon$.

Examining the threshold choices in Theorems 5.4 and 5.5 reveals a key property: hard clipping C_τ leaves any coordinate within the range of the true gradient unaltered, while smooth shrinkage S_c requires a larger threshold to preserve ordinary signals and control the Cauchy tail. In both cases, the threshold remains *constant* once the noise scale and gradient bounds are established, complementary to existing clipping methods that require iteration-dependent thresholds [9].

5.2 Convergence Result for Pre-clipping

Given an entry-wise mapping $\varphi : \mathbb{R}^{m \times n} \rightarrow \mathbb{R}^{m \times n}$, we consider the following mini-batched pre-clipping using N *i.i.d.* samples:

$$\tilde{G}_k^\varphi := \frac{1}{N} \sum_{\ell=1}^N \varphi(G_k + \Xi_k^{(\ell)}), \quad X_{k+1} = X_k - \eta \text{msign}(\tilde{G}_k^\varphi), \quad (17)$$

where $\text{msign}(M) = UV^T$ for the singular value decomposition $M = U\Sigma V^T$. We define $r := \min\{m, n\}$, $q := \max\{m, n\}$, and $D := \sqrt{q/r}$. The subsequent theorems establish convergence guarantees when φ is instantiated as either C_τ or S_c .

Theorem 5.6 (Pre-clipped Muon with hard clipping). *Under Assumptions 5.1 to 5.3, choose τ such that $\tau \geq B + \max\left\{\sigma\sqrt{2\log(16\sqrt{r})}, \frac{16\alpha\gamma\sqrt{r}}{\pi}\right\}$, and define $v_\tau := (1 - \alpha)\sigma^2 + \frac{4\alpha\gamma\tau}{\pi}$.*

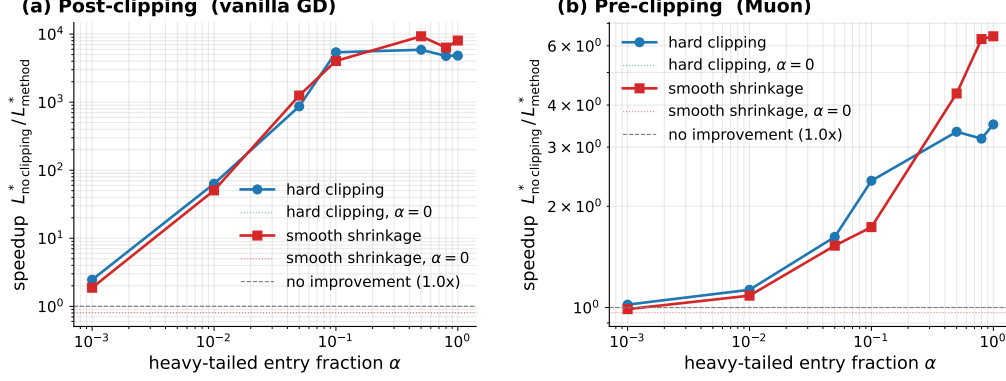


Figure 3: Random Gaussian feature regression ($d = 32$, $n = 128$) with a fraction α of feature entries corrupted by Student- t noise ($\nu = 1$, scale 3.0). y -axis is the final-loss speedup over no clipping. Smooth shrinkage (red) in both *post-clipping* (a) and *pre-clipping* (b) tracks hard clipping (blue) for small α but pulls ahead as the noise is dominated by heavy-tailed entries.

Executing the update rule Equation (17) with $\varphi = C_\tau$ and a step size of $\eta = \sqrt{2\Delta/(LrT)}$ for T iterations yields:

$$\frac{1}{T} \sum_{k=0}^{T-1} \mathbb{E} \|G_k\|_* \leq 2\sqrt{\frac{2Lr\Delta}{T}} + 4Dr^{3/2} \sqrt{\frac{v_\tau}{N}}. \quad (18)$$

Consequently, for $T \geq 32Lr\Delta/\varepsilon^2$ and $N \geq 64D^2r^3v_\tau/\varepsilon^2$, we guarantee $\frac{1}{T} \sum_{k=0}^{T-1} \mathbb{E} \|G_k\|_* \leq \varepsilon$.

Theorem 5.7 (Pre-clipped Muon with smooth shrinkage). *Under Assumptions 5.1 to 5.3, choose $c \geq \max \left\{ 8\sqrt{r} \left[B + \sqrt{\frac{8}{\pi}}(1-\alpha)\sigma \right], \frac{128\alpha\gamma\sqrt{r}}{\pi} \log \left(e + \frac{128\alpha\sqrt{r}}{\pi} \right) \right\}$, and define $v_c := (1-\alpha)\sigma^2 + \frac{8\alpha\gamma c}{\pi e}$. Executing the update rule Equation (17) with $\varphi = S_c$ and a step size of $\eta = \sqrt{2\Delta/(LrT)}$ for T iterations yields:*

$$\frac{1}{T} \sum_{k=0}^{T-1} \mathbb{E} \|G_k\|_* \leq 2\sqrt{\frac{2Lr\Delta}{T}} + 4Dr^{3/2} \sqrt{\frac{v_c}{N}}. \quad (19)$$

Consequently, for $T \geq 32Lr\Delta/\varepsilon^2$ and $N \geq 64D^2r^3v_c/\varepsilon^2$, we guarantee $\frac{1}{T} \sum_{k=0}^{T-1} \mathbb{E} \|G_k\|_* \leq \varepsilon$.

The heavy tail enters the constants, not the exponent. Under the explicit noise model in Assumption 5.3, despite the raw oracle \tilde{G} having no first absolute moment, all four rates retain the standard $\mathcal{O}(\varepsilon^{-4})$ accuracy dependence: the Cauchy heavy tail is absorbed into the threshold and variance constants, not into the complexity exponent. This is possible because our noise is an entry-wise *symmetric location* perturbation around the clean gradient, enabling us to derive the *multiplicative* bias bound $|\mathbb{E}[\varphi(g + \xi)] - g| \leq \rho|g|$ after some clipping map φ . On the contrary, the asymmetric finite \mathfrak{p} -moment assumption for the stochastic gradient noise [9, 17, 26, 27], instead gives an *additive* bias bound of the form $|\mathbb{E}[\varphi(g + \xi) - g]| \leq C\sigma^{\mathfrak{p}}/\tau^{\mathfrak{p}-1}$ with the rate degrading as the tail becomes heavier (i.e., as $\mathfrak{p} \rightarrow 1$). We present detailed proofs of the above theorems in Section E.

6 Experiments

Random Gaussian feature regression. We minimize $L(W) = \frac{1}{2n} \|WA - Y\|_F^2$ with i.i.d. Gaussian features A , where gradients are corrupted by the contamination model in Equation (6) with Cauchy heavy tails ($H = t_1$). We want to investigate how entry-wise

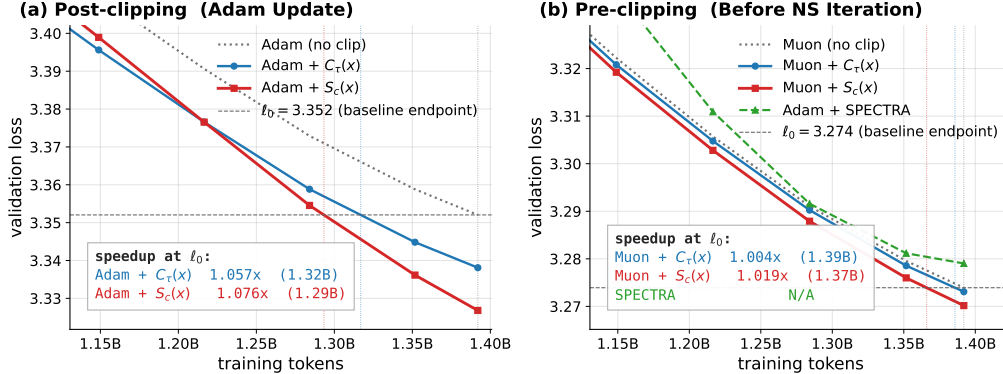


Figure 4: Validation loss vs. tokens on Modded-NanoGPT under hard clipping ($C_\tau(x)$) and smooth shrinkage ($S_c(x)$). ℓ_0 is the no-clipping baseline’s final loss; speedup := $\text{tokens}_{\text{baseline}}/\text{tokens}_{\text{methods}}$ with linear interpolation between eval points. Smooth shrinkage improves Adam and Muon on NanoGPT through saving $\sim 7.6\%$ and $\sim 1.9\%$ training tokens respectively.

clipping can speed up vanilla GD and spectral GD from post-clipping and pre-clipping under hard clipping and smooth shrinkage operators. We report the median of the minimized loss in Figure 3 after a grid search over learning rate and clipping threshold under a fixed number of iteration steps. We observe that both entry-wise methods barely have any speedup when the noise is dominated by Gaussian, consistent with the findings in [28]. However, as the noise progresses into the heavy-tailed region, smooth shrinkage starts to outperform hard clipping, especially when it enters into a heavy-tail dominated region ($\alpha > 0.5$). We further observe that both clipping methods help recover the spiked spectral structure and rotated subspace corrupted by heavy-tailed noise, as shown in Figures 6 to 9(a). This provides an explanation for why clipping is beneficial at the pre-clipping stage. We provide the full setup and additional results in Section F.1.

Language model pretraining. In this section, we investigate the benefits of entry-wise clipping for language modeling tasks under two different clipping stages. We use the modded-nanoGPT codebase [29], where it is equipped with rotary embeddings, RMSNorm, linear decay learning-rate schedule, ReLU² activations, three value-embedding layers, and an untied output head, totalling 276M parameters. We pretrain it on FineWeb [30]. We report validation loss curves under each method’s best learning rate and clipping threshold in Figure 4, and observe that the proposed smooth shrinkage operator improves Adam and Muon by saving $\sim 7.6\%$ and $\sim 1.9\%$ of training tokens, respectively. We conjecture the reason why smooth shrinkage outperforms hard clipping is that large-scale language data often contains rare tokens that can easily fall into the heavy-tailed region where smooth shrinkage has a better performance. We provide the detailed experiment settings and hyperparameter sweeping result in Section F.2.

7 Conclusion

In this work, we studied whether entry-wise clipping can provide a computationally cheap mechanism for controlling the spectrum of stochastic matrix gradients under heavy-tailed noise. Motivated by empirical observations from language model pretraining, we showed that real stochastic gradient noise exhibits an entry-wise heavy-tailed and localized structure, in which a small number of large entries can dominate spectral perturbations. To formalize this phenomenon, we introduced a localization ratio derived from first-order singular-value perturbation analysis, which identifies regimes where entry-wise operations can effectively

influence spectral behavior.

Building on this observation, we proposed smooth shrinkage, a Bayes-motivated entry-wise clipping operator designed to suppress heavy-tailed contamination while preserving ordinary signal components. Unlike hard coordinate-wise clipping, smooth shrinkage applies an exponentially decaying retention factor, yielding stronger suppression of extreme entries. We established convergence guarantees for both hard clipping and smooth shrinkage under Cauchy-contaminated noise, showing that the heavy-tailed component affects only the constants rather than the standard $\mathcal{O}(\varepsilon^{-4})$ complexity exponent. Finally, our experiments demonstrate that smooth shrinkage improves both post-clipping and pre-clipping regimes: it accelerates Adam in NanoGPT pretraining and yields additional gains when applied before Muon-style spectral normalization.

References

- [1] Keller Jordan, Yuchen Jin, Vlado Boza, Jiacheng You, Franz Cesista, Laker Newhouse, and Jeremy Bernstein. *Muon: An optimizer for hidden layers in neural networks*. 2024. URL: <https://kellerjordan.github.io/posts/muon/> (cit. on pp. 1, 4, 17, 43).
- [2] Umut Simsekli, Levent Sagun, and Mert Gurbuzbalaban. “A tail-index analysis of stochastic gradient noise in deep neural networks”. In: *International Conference on Machine Learning*. PMLR. 2019, pp. 5827–5837 (cit. on pp. 1, 5, 17).
- [3] Mert Gurbuzbalaban, Umut Simsekli, and Lingjiong Zhu. “The heavy-tail phenomenon in SGD”. In: *International Conference on Machine Learning*. PMLR. 2021, pp. 3964–3975 (cit. on p. 1).
- [4] Aaron Grattafiori, Abhimanyu Dubey, Abhinav Jauhri, Abhinav Pandey, Abhishek Kadian, Ahmad Al-Dahle, Aiesha Letman, Akhil Mathur, Alan Schelten, Alex Vaughan, et al. “The llama 3 herd of models”. In: *arXiv preprint arXiv:2407.21783* (2024) (cit. on p. 1).
- [5] Kimi Team, Yifan Bai, Yiping Bao, Y Charles, Cheng Chen, Guanduo Chen, Haiting Chen, Huarong Chen, Jiahao Chen, Ningxin Chen, et al. “Kimi k2: Open agentic intelligence”. In: *arXiv preprint arXiv:2507.20534* (2025) (cit. on pp. 1, 43).
- [6] Mitchell Wortsman, Peter J Liu, Lechao Xiao, Katie E Everett, Alexander A Alemi, Ben Adlam, John D Co-Reyes, Izzeddin Gur, Abhishek Kumar, Roman Novak, Jeffrey Pennington, Jascha Sohl-Dickstein, Kelvin Xu, Jaehoon Lee, Justin Gilmer, and Simon Kornblith. “Small-scale proxies for large-scale Transformer training instabilities”. In: *The Twelfth International Conference on Learning Representations*. 2024 (cit. on p. 1).
- [7] Tianjin Huang, Ziquan Zhu, Gaojie Jin, Lu Liu, Zhangyang Wang, and Shiwei Liu. “SPAM: Spike-aware adam with momentum reset for stable LLM training”. In: *The Thirteenth International Conference on Learning Representations*. 2025 (cit. on p. 1).
- [8] Razvan Pascanu, Tomas Mikolov, and Yoshua Bengio. “On the difficulty of training recurrent neural networks”. In: *International conference on machine learning*. Pmlr. 2013, pp. 1310–1318 (cit. on pp. 1, 4, 17).
- [9] Jingzhao Zhang, Sai Praneeth Karimireddy, Andreas Veit, Seungyeon Kim, Sashank Reddi, Sanjiv Kumar, and Suvrit Sra. “Why are adaptive methods good for attention models?” In: *Advances in Neural Information Processing Systems* 33 (2020), pp. 15383–15393 (cit. on pp. 1, 4, 5, 9, 10, 17).
- [10] David Carlson, Volkan Cevher, and Lawrence Carin. “Stochastic spectral descent for restricted Boltzmann machines”. In: *Artificial intelligence and statistics*. PMLR. 2015, pp. 111–119 (cit. on pp. 1, 17).
- [11] Takeru Miyato, Toshiki Kataoka, Masanori Koyama, and Yuichi Yoshida. “Spectral normalization for generative adversarial networks”. In: *International Conference on Learning Representations*. 2018 (cit. on p. 1).
- [12] Kaiyue Wen, David Leo Wright Hall, Tengyu Ma, and Percy Liang. “Fantastic Pre-training Optimizers and Where to Find Them”. In: *The Fourteenth International Conference on Learning Representations*. 2026 (cit. on p. 1).
- [13] Jeremy Bernstein and Laker Newhouse. “Old optimizer, new norm: An anthology”. In: *arXiv preprint arXiv:2409.20325* (2024) (cit. on pp. 1, 17).
- [14] Xiaowen Jiang, Andrei Semenov, and Sebastian U Stich. “Enhancing LLM Training via Spectral Clipping”. In: *arXiv preprint arXiv:2603.14315* (2026) (cit. on pp. 1, 4, 5, 17, 43).
- [15] Laker Newhouse, R Preston Hess, Franz Cesista, Andrii Zahorodnii, Jeremy Bernstein, and Phillip Isola. “Training transformers with enforced lipschitz constants”. In: *arXiv preprint arXiv:2507.13338* (2025) (cit. on pp. 4, 17).

- [16] Ashok Cutkosky and Harsh Mehta. “High-probability bounds for non-convex stochastic optimization with heavy tails”. In: *Advances in Neural Information Processing Systems* 34 (2021), pp. 4883–4895 (cit. on pp. 4, 17).
- [17] Ta Duy Nguyen, Thien Hang Nguyen, Alina Ene, and Huy Nguyen. “Improved Convergence in High Probability of Clipped Gradient Methods with Heavy Tailed Noise”. In: *Thirty-seventh Conference on Neural Information Processing Systems. 2023* (cit. on pp. 4, 10, 17).
- [18] Chongjie Si, Debing Zhang, and Wei Shen. “Adamuon: Adaptive muon optimizer”. In: *arXiv preprint arXiv:2507.11005* (2025) (cit. on p. 4).
- [19] Wei He, Kai Han, Hang Zhou, Hanting Chen, Zhicheng Liu, Xinghao Chen, and Yunhe Wang. “ROOT: Robust Orthogonalized Optimizer for Neural Network Training”. In: *arXiv preprint arXiv:2511.20626* (2025) (cit. on p. 4).
- [20] Sandrine Péché. “The largest eigenvalue of small rank perturbations of Hermitian random matrices”. In: *Probability Theory and Related Fields* 134.1 (2006), pp. 127–173 (cit. on p. 5).
- [21] Peter J Huber. “Robust estimation of a location parameter”. In: *Breakthroughs in statistics: Methodology and distribution*. Springer, 1992, pp. 492–518 (cit. on p. 5).
- [22] Steven T Piantadosi. “Zipf’s word frequency law in natural language: A critical review and future directions”. In: *Psychonomic bulletin & review* 21.5 (2014), pp. 1112–1130 (cit. on p. 5).
- [23] George Kingsley Zipf. *Human behavior and the principle of least effort: An introduction to human ecology*. Ravenio books, 2016 (cit. on p. 5).
- [24] Jan R Magnus. “On differentiating eigenvalues and eigenvectors”. In: *Econometric theory* 1.2 (1985), pp. 179–191 (cit. on pp. 5, 20).
- [25] Tosio Kato. *Perturbation theory for linear operators*. Vol. 132. Springer, 1966 (cit. on pp. 5, 20).
- [26] Liam Madden, Emiliano Dall’Anese, and Stephen Becker. “High probability convergence bounds for non-convex stochastic gradient descent with sub-weibull noise”. In: *Journal of Machine Learning Research* 25.241 (2024), pp. 1–36 (cit. on p. 10).
- [27] Zijian Liu and Zhengyuan Zhou. “Nonconvex stochastic optimization under heavy-tailed noises: Optimal convergence without gradient clipping”. In: *The Thirteenth International Conference on Learning Representations*. 2025 (cit. on pp. 10, 17).
- [28] Noah Marshall, Ke Liang Xiao, Atish Agarwala, and Elliot Paquette. “To clip or not to clip: the dynamics of SGD with gradient clipping in high-dimensions”. In: *International Conference on Learning Representations*. Vol. 2025. 2025, pp. 27381–27417 (cit. on p. 11).
- [29] Keller Jordan, Jeremy Bernstein, Brendan Rappazzo, @fernbear.bsky.social, Boza Vlado, You Jiacheng, Franz Cesista, Braden Koszarsky, and @Grad62304977. *modded-nanogpt: Speedrunning the NanoGPT baseline*. 2024. URL: <https://github.com/KellerJordan/modded-nanogpt> (cit. on pp. 11, 43).
- [30] Guilherme Penedo, Hynek Kydlíček, Anton Lozhkov, Margaret Mitchell, Colin Raffel, Leandro Von Werra, Thomas Wolf, et al. “The fineweb datasets: Decanting the web for the finest text data at scale”. In: *Advances in Neural Information Processing Systems* 37 (2024), pp. 30811–30849 (cit. on pp. 11, 43).
- [31] Thomas Pethick, Wanyun Xie, Mete Erdogan, Kimon Antonakopoulos, Tony Silveti-Falls, and Volkan Cevher. “Generalized Gradient Norm Clipping & Non-Euclidean (L_0, L_1) -Smoothness”. In: *The Thirty-ninth Annual Conference on Neural Information Processing Systems*. 2025 (cit. on p. 17).

- [32] Maria-Eleni Sfyraiki and Jun-Kun Wang. “Lions and muons: Optimization via stochastic frank-wolfe”. In: *arXiv preprint arXiv:2506.04192* (2025) (cit. on p. 17).
- [33] Aleksandar Armacki, Pranay Sharma, Gauri Joshi, Dragana Bajovic, Dusan Jakovetic, and Soumya Kar. “High-probability convergence bounds for nonlinear stochastic gradient descent under heavy-tailed noise”. In: *Proceedings of The 28th International Conference on Artificial Intelligence and Statistics*. 2025 (cit. on p. 17).
- [34] Yurii E Nesterov. “Minimization methods for nonsmooth convex and quasiconvex functions”. In: *Matekon* 29.3 (1984), pp. 519–531 (cit. on p. 17).
- [35] Yurii Nesterov et al. *Lectures on convex optimization*. Vol. 137. Springer, 2018 (cit. on p. 17).
- [36] Zijian Liu, Jiawei Zhang, and Zhengyuan Zhou. “Breaking the lower bound with (little) structure: Acceleration in non-convex stochastic optimization with heavy-tailed noise”. In: *The Thirty Sixth Annual Conference on Learning Theory*. PMLR. 2023, pp. 2266–2290 (cit. on p. 17).
- [37] Florian Hübler, Ilyas Fatkhullin, and Niao He. “From gradient clipping to normalization for heavy tailed sgd”. In: *arXiv preprint arXiv:2410.13849* (2024) (cit. on p. 17).
- [38] Jeremy Bernstein, Yu-Xiang Wang, Kamyar Azizzadenesheli, and Animashree Anandkumar. “signSGD: Compressed optimisation for non-convex problems”. In: *International conference on machine learning*. PMLR. 2018, pp. 560–569 (cit. on p. 17).
- [39] Xinyu Luo, Cedar Site Bai, Bolian Li, Petros Drineas, Ruqi Zhang, and Brian Bullins. “Stacey: Promoting Stochastic Steepest Descent via Accelerated ℓ_p -Smooth Nonconvex Optimization”. In: *Forty-second International Conference on Machine Learning*. 2025 (cit. on p. 17).
- [40] Wei Shen, Ruichuan Huang, Minhui Huang, Cong Shen, and Jiawei Zhang. “On the convergence analysis of muon”. In: *arXiv preprint arXiv:2505.23737* (2025) (cit. on p. 17).
- [41] Zitao Song, Cedar Site Bai, Zhe Zhang, Brian Bullins, and David F Gleich. “Decoupling Variance and Scale-Invariant Updates in Adaptive Gradient Descent for Unified Vector and Matrix Optimization”. In: *Forty-third International Conference on Machine Learning*. 2026 (cit. on p. 17).
- [42] Diederik P Kingma and Jimmy Ba. “Adam: A method for stochastic optimization”. In: *arXiv preprint arXiv:1412.6980* (2014) (cit. on p. 17).
- [43] Nicholas G Polson and James G Scott. “Shrink globally, act locally: Sparse Bayesian regularization and prediction”. In: *Bayesian statistics* 9.501-538 (2010), p. 105 (cit. on p. 24).
- [44] Anthony O’Hagan. “On outlier rejection phenomena in Bayes inference”. In: *Journal of the Royal Statistical Society Series B: Statistical Methodology* 41.3 (1979), pp. 358–367 (cit. on p. 24).
- [45] LR Pericchi and AFM Smith. “Exact and approximate posterior moments for a normal location parameter”. In: *Journal of the Royal Statistical Society Series B: Statistical Methodology* 54.3 (1992), pp. 793–804 (cit. on p. 24).
- [46] Ilya Loshchilov and Frank Hutter. “Decoupled weight decay regularization”. In: *International Conference on Learning Representations*. 2019 (cit. on p. 43).
- [47] Shengding Hu, Yuge Tu, Xu Han, Chaoqun He, Ganqu Cui, Xiang Long, Zhi Zheng, Yewei Fang, Yuxiang Huang, Weilin Zhao, et al. “Minicpm: Unveiling the potential of small language models with scalable training strategies”. In: *First Conference on Language Modeling*. 2024 (cit. on p. 43).

Appendix

Contents

1	Introduction	1
2	Preliminaries	2
2.1	Clipping Methods for Gradient Updates	2
2.2	Stages for Gradient Clipping	4
3	Heavy-tailed Entries Can Drive Spectral Inflation	4
3.1	Subspace Perturbation vs. Entry-wise Contamination	5
3.2	From First-order Perturbation to a Localization Metric	5
3.3	From Localization to Entry-wise Minimization	6
4	Smooth Shrinkage: A Bayes-Motivated Entry-Wise Spectrum Control	7
5	Convergence Analysis	8
5.1	Convergence Result for Post-clipping	8
5.2	Convergence Result for Pre-clipping	9
6	Experiments	10
7	Conclusion	11
A	Related Work	17
B	Additional Information for Smooth Shrinkage and Limitations	18
C	Proofs for Section 3	20
C.1	Proof of Theorem 3.3	20
D	Proofs for Section 4	23
D.1	Proof of Theorem 4.1	23
D.2	Proof of Lemma D.3	24
E	Proofs for Section 5	27
E.1	Elementary Scalar Inequalities	28
E.2	Proofs of Scalar Relative bias and Variance under C_τ	29
E.3	Proofs of Scalar Relative bias and Variance under S_c	30
E.4	Proofs of Clipping Threshold τ and c	32
E.5	Proofs of Theorems 5.4 and 5.5	34
E.6	Proofs of Theorems 5.6 and 5.7	35
F	Experiment Details for Section 6	38
F.1	Gaussian Random Feature Regression	38
F.2	Language Model Pretraining	43

Appendix

A Related Work

Gradient Clipping Methods. Global gradient clipping is widely used to stabilize training in deep learning [8]. When the stochastic gradient noise is heavy-tailed [2], under the assumption of an unbiased gradient oracle with finite p -th central moment for some $p \in (1, 2]$, Zhang et al. [9] first established the $\Omega(T^{\frac{1-p}{3p-2}})$ lower bound for nonconvex optimization; Zhang et al. [9] and Nguyen et al. [17] respectively provided matching in-expectation and high-probability upper bounds for clipped SGD, up to extra logarithmic factors. These analyses, however, rely on iteration-dependent clipping thresholds, e.g. $c_t = c \cdot t^{\frac{1}{3p-2}}$.

Beyond the global clipping variants, under coordinate-wise heavy-tailed noise, coordinate-wise clipping has been shown to converge faster than global clipping for μ -strongly convex objectives [9]. More recently, global clipping has been extended to non-Euclidean space in the context of large-scale language model training [14, 31]: under a standard bounded-variance noise model, an $\mathcal{O}(T^{-1/4})$ rate was established within a Frank-Wolfe analysis framework [31], and Sfyraiki and Wang [32] obtained a high probability $\tilde{\mathcal{O}}(T^{\frac{1-p}{3p-2}})$ rate under the bounded p -th moment assumption. Nonetheless, little is known about how clipping behaves in the unbounded-noise regime ($p = 1$), even when the noise density distribution is known [33].

Normalized Methods. Normalized gradient methods [34, 35] are another line of research that controls gradient noise without requiring an iteration-dependent clipping threshold. Under the Euclidean norm and a finite p -th moment assumption on the noise, Cutkosky and Mehta [16] and Liu, Zhang, and Zhou [36] study variants of normalized SGD that incorporate gradient clipping as an additional ingredient. More recently, Hübler, Fatkhullin, and He [37] and Liu and Zhou [27] have shown that normalized SGD attains the optimal complexity $\mathcal{O}(T^{\frac{1-p}{3p-2}})$ in the nonconvex setting *without* any clipping. Beyond the Euclidean geometry, under a standard bounded-variance gradient oracle, SignSGD [38] and Stacey [39] have been shown to achieve an $\mathcal{O}(T^{-1/4})$ rate with stationarity measured in the ℓ_1 and ℓ_{p^*} (dual) norms, respectively, in the nonconvex setting. Most recently, spectral-norm normalization (i.e., Muon-type updates) has likewise been shown to attain the $\mathcal{O}(T^{-1/4})$ complexity under bounded variance [40].

Spectral Methods. Among normalized methods, spectral-norm methods [1, 10, 13] respect the matrix structure of large-scale neural networks and have emerged as an alternative to optimizers that flatten weights into long vectors. Within this spectral geometry, one can develop adaptive spectral methods [41] and spectral clipping methods [14, 15], in direct analogy to Adam [42] and global gradient clipping in the adaptive vector optimizer or vector clipping setting. Nevertheless, how coordinate-wise gradient clipping affects the spectrum of the weight matrices remains largely unexplored.

B Additional Information for Smooth Shrinkage and Limitations

In this section, we provide additional details and a reference implementation of smooth shrinkage. Figure 5 compares its damping factor $e^{-|y|/\tau}$ against the hard clipping factor $\min\{1, c/|y|\}$.

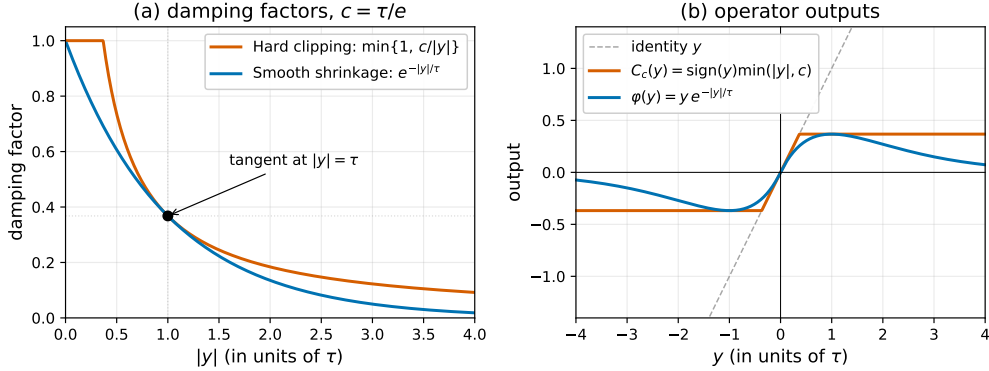


Figure 5: Comparison of smooth shrinkage and hard coordinate-wise clipping at the tangent calibration $c = \tau/e$. **(a)** Damping factors $e^{-|y|/\tau}$ and $\min\{1, c/|y|\}$ meet tangentially at $|y| = \tau$ with value $1/e$. **(b)** Operator outputs: hard clipping plateaus at magnitude c , while smooth shrinkage peaks near $|y| = \tau$ and decays exponentially, imposing a strictly stronger penalty on large entries.

We present the implementation below, which adds only two lines to the original optimizer code.

```
def smooth_shrinkage(x, q):
    c = torch.quantile(x.abs(), q)
    return x * torch.exp(-x.abs() / c.clamp(min=1e-12))

# ---- Post-clipping: apply phi to any optimizer update direction U ----
U = ... # e.g., AdamW: m / (v.sqrt() + eps)
U = smooth_shrinkage(U, q)
W -= lr * U

# ---- Pre-clipping: apply phi to any signal S before matrix-sign ----
S = ... # e.g., momentum m, raw gradient g, ...
S = smooth_shrinkage(S, q)
W -= lr * scale * msign(S) # scale = 0.2 * sqrt(max(n, m))
```

Broader Impacts This work contributes algorithmic improvements to the optimization of matrix-valued weights in large-scale neural network training. The direct positive consequence is improved compute and energy efficiency: token savings of $\sim 7\%$ for Adam and $\sim 2\%$ for Muon during NanoGPT pretraining translate to proportional reductions in resource cost and carbon footprint at scale, with potential to broaden access for compute-constrained research groups.

Limitations The derivation of the above smooth shrinkage in Theorem 4.1 places a Gaussian prior $G_{ij} \stackrel{\text{iid}}{\sim} \mathcal{N}(0, \sigma_x^2)$ on the clean gradient signal. While the entrywise contamination model (Definition 3.2) captures heavy-tailed fluctuations, the assumption that the underlying

full-batch gradient has a Gaussian-like bulk is a modeling choice rather than an empirical fact. Structured signals aligned with task-specific low-rank subspaces may violate it and shift the form of the optimal entrywise estimator. In addition, the dichotomy between entrywise heavy-tailed contamination and bounded-second-moment subspace perturbation does not exhaust the relevant alternatives: an anisotropic low-rank perturbation without bounded second moment can itself induce heavy-tailed spectral structure, and a unified analysis of this is more involved and thus left to future work.

C Proofs for Section 3

C.1 Proof of Theorem 3.3

Theorem 3.3 (First-order expansion of σ_1). *Let $G \in \mathbb{R}^{m \times n}$ have a simple top singular value $\sigma_1(G) > \sigma_2(G)$, with corresponding left and right singular vectors u_1 and v_1 , and let $\delta := \sigma_1(G) - \sigma_2(G)$ denote the spectral gap. There exists a universal constant $C > 0$ such that for every perturbation $E \in \mathbb{R}^{m \times n}$ with $\|E\|_{op} < \delta/4$,*

$$\sigma_1(G + E) = \sigma_1(G) + \sum_{ij} (u_1)_i (v_1)_j E_{ij} + \theta, \quad |\theta| \leq C \frac{\|E\|_{op}^2}{\delta}. \quad (7)$$

Remark C.1. The bilinear first-order coefficient $u_1^T E v_1$ is classical and goes back to Magnus [24]; analytic perturbation theory for simple eigenvalues of symmetric matrices is developed in Kato [25, Ch. II]. The Taylor expansion in the form of Equation (7), together with an explicit quadratic remainder, is not stated in those references, so we provide a self-contained proof in the following section.

Proof of Theorem 3.3.

Symmetric reduction Define the symmetric block matrices

$$A := \begin{pmatrix} 0 & G \\ G^T & 0 \end{pmatrix}, \quad B := \begin{pmatrix} 0 & E \\ E^T & 0 \end{pmatrix} \in \mathbb{R}^{(m+n) \times (m+n)},$$

and set $N := m + n$. The spectrum of A is $\{\pm \sigma_k(G)\}_{k=1}^{\min(m,n)} \cup \{0, \dots, 0\}$, with $2|m - n|$ zero eigenvalues. The hypothesis $\sigma_1(G) > \sigma_2(G) \geq 0$ implies that $\lambda_* := \lambda_1(A) = \sigma_1(G)$ is a simple eigenvalue with unit eigenvector $w_* := \frac{1}{\sqrt{2}} \begin{pmatrix} u_1 \\ v_1 \end{pmatrix}$, and the gap between the top two eigenvalues of A equals δ . A direct computation gives $\|B\|_{op} = \|E\|_{op}$ and $\sigma_1(G + E) = \lambda_1(A + B)$, so it suffices to establish the expansion for λ_1 .

Local differentiability of $\lambda(\cdot)$ and $w(\cdot)$ Here we show the differentiability of $\lambda(\cdot)$ and $w(\cdot)$ along the perturbation direction via the Implicit Function Theorem.

Let $S \in \text{Sym}(N)$ be a N by N symmetric perturbation to the matrix A , the eigenvalue problem of on perturbed matrix $A + S$ defines a S parameterized smooth map $F : \mathbb{R} \times \mathbb{R}^N \times \text{Sym}(N) \rightarrow \mathbb{R} \times \mathbb{R}^N$:

$$F(\lambda, w; S) = \left((A + S - \lambda I) w, \frac{1}{2}(\|w\|^2 - 1) \right), \text{ where } \lambda \in \mathbb{R}, w \in \mathbb{R}^N.$$

Recall λ_* and w_* are the eigenvalue and eigenvectors of A , when $S = 0$, we have $F(\lambda_*, w_*, 0) = 0$. We denote $(a, v) \in \mathbb{R} \times \mathbb{R}^N$ as the local perturbation at (λ_*, w_*) . The Jacobian of $F(\lambda, w)$ at this point with can be written as

$$L(a, v) = \begin{pmatrix} -w_* & A - \lambda_* I \\ 0 & w_* \end{pmatrix} \begin{pmatrix} a \\ v \end{pmatrix}.$$

We claim $L(a, v) = 0$ only has trivial solution. If $L(a, v) = 0$, then $v \perp w_*$ and $aw_* = (A - \lambda_* I)v$. Taking the inner product with w_* to the second equation and using symmetry,

$$a = w_*^T (A - \lambda_* I)v = ((A - \lambda_* I)w_*)^T v = 0.$$

Hence $(A - \lambda_* I)v = 0$, so $v \in \ker(A - \lambda_* I) = \text{span}(w_*)$. Since λ_* is simple and there is no repetitive eigenvalue, combined with $v \perp w_*$, this forces $v = 0$. Then the Jacobian matrix $\begin{pmatrix} -w_* & A - \lambda_* I \\ 0 & w_* \end{pmatrix}$ is invertible.

Since F is C^∞ , by the implicit function theorem there exists a neighborhood $U \subset \text{Sym}(N)$ around 0 and a unique C^∞ map $D_{(\lambda,w)}F : S \mapsto (\lambda(S), w(S))$ on U with $D_{(\lambda,w)}F(0) = (\lambda_*, w_*)$ and $F(\lambda(S), w(S); S) = 0$.

Local differentiability extension. Now, we want to extend the local differentiability from the neighborhood $U \in \text{Sym}(N)$ around 0 to all perturbations B that satisfy $\|B\|_{op} < \delta/4$.

Parametrize the segment $t \mapsto A + tB$ for $t \in [0, 1]$. By Weyl's inequality, $|\lambda_k(A + tB) - \lambda_k(A)| \leq t \|B\|_{op}$ for every k , so

$$\delta(t) := \lambda_1(A + tB) - \lambda_2(A + tB) \geq \delta - 2t \|B\|_{op} \geq \delta - 2 \|B\|_{op} > 0$$

for all $t \in [0, 1]$. The top eigenvalue of $A + tB$ stays simple along the segment, so the IFT applies at each $t \in [0, 1]$. A connectedness argument (the set of $t \in [0, 1]$ for which a smooth branch $((\lambda(t), w(t)))$ exists is open, closed, and nonempty) can promote our previous local statement from the IFT to 'global' one along the line segment, this yields a C^∞ function

$$f : [0, 1] \rightarrow \mathbb{R}, \quad f(t) := \lambda_1(A + tB),$$

together with a C^∞ unit eigenvector path $w : [0, 1] \rightarrow \mathbb{R}^N$ satisfying $(A + tB)w(t) = f(t)w(t)$ and $\|w(t)\| = 1$.

First derivative derivation. Now with the differentiability along the line segment, Differentiating the following perturbed eigenvalue problem with respect to t

$$(A + tB)w(t) = f(t)w(t),$$

this yields

$$Bw(t) + (A + tB - f(t)I)w'(t) = f'(t)w(t). \quad (20)$$

Taking the inner product with $w(t)$ and using both the symmetry of $A + tB$ and the eigenvector identity $(A + tB - f(t)I)w(t) = 0$,

$$f'(t) = w(t)^T B w(t). \quad (21)$$

At $t = 0$ this gives $f'(0) = w_*^T B w_*$. Substituting $w_* = \frac{1}{\sqrt{2}} \begin{pmatrix} u_1 \\ v_1 \end{pmatrix}$ and the block form of B ,

$$w_*^T B w_* = \frac{1}{2} (u_1^T, v_1^T) \begin{pmatrix} 0 & E \\ E^T & 0 \end{pmatrix} \begin{pmatrix} u_1 \\ v_1 \end{pmatrix} = \frac{1}{2} (u_1^T E v_1 + v_1^T E^T u_1) = u_1^T E v_1,$$

which is the claimed first order coefficient $\sum_{i,j} (u_1)_i (v_1)_j E_{ij}$.

Second derivative bound. Now we want to bound the second-order derivative of $f(t)$. Differentiating Equation (21) and using the symmetry of B we have

$$f''(t) = 2w(t)^T B w'(t) \quad (22)$$

$$\leq 2\|B\|_{op}\|w'(t)\|. \quad (23)$$

The second inequality follows by Cauchy and $\|w(t)\| = 1$. Now we want to bound the term $w'(t)$.

Differentiating $\|w(t)\|^2 = 1$ gives $w(t)^T w'(t) = 0$, so $w'(t) \in w(t)^\perp$. Rearranging Equation (20) yields

$$(A + tB - f(t)I)w'(t) = (f'(t)I - B)w(t).$$

The right hand side lies in $w(t)^\perp$, since $w(t)^T (f'(t)I - B)w(t) = f'(t) - w(t)^T B w(t) = 0$ by Equation (21). Since $\delta(t) > 0$, $A + tB - f(t)I$ restricted to the orthogonal complement $w(t)^\perp$

is invertible, and its inverse has operator norm bounded by $1/\delta(t)$. Since $w'(t) \in w(t)^\perp$, we have

$$\begin{aligned}
\|w'(t)\| &\leq \|(A + tB - f(t)I)^{-1}\|_{op} \|(f'(t)I - B)w(t)\| \\
&\leq \frac{\|(f'(t)I - B)w(t)\|}{\delta(t)} \\
&= \frac{\|Bw(t) - (w(t)^T B w(t))w(t)\|}{\delta(t)} \\
&\leq \frac{\|Bw(t)\|}{\delta(t)} \\
&\leq \frac{\|B\|_{op}}{\delta - 2\|B\|_{op}},
\end{aligned}$$

where the third inequality follows from the orthogonal decomposition of $Bw(t)$ along $w(t)$ and $w(t)^\perp$, which gives $\|Bw - (w^T B w)w\|^2 = \|Bw\|^2 - |w^T B w|^2 \leq \|Bw\|^2$. When $\|B\|_{op} \leq \delta/4$, combining with Equation (23),

$$|f''(t)| \leq 2\|B\|_{op}\|w'(t)\| \leq \frac{2\|B\|_{op}^2}{\delta - 2\|B\|_{op}} \leq \frac{4\|B\|_{op}^2}{\delta} \quad \text{for all } t \in [0, 1]. \quad (24)$$

Taylor with remainder. By Taylor's theorem in one real variable applied to f on $[0, 1]$, there exists $\xi \in (0, 1)$ such that

$$f(1) = f(0) + f'(0) + \frac{1}{2}f''(\xi).$$

Set $\theta(E) := \frac{1}{2}f''(\xi)$. The bound Equation (24) gives $|\theta(E)| \leq \frac{4\|B\|_{op}^2}{\delta}$. Translating back via $f(1) = \lambda_1(A + B) = \sigma_1(G + E)$, $f(0) = \sigma_1(G)$, $f'(0) = u_1^T E v_1$, and $\|B\|_{op} = \|E\|_{op}$ delivers Equation (7). \square

D Proofs for Section 4

Throughout this section, we use ϕ_{σ_x} to denote the density of $\mathcal{N}(0, \sigma_x^2)$, h as the density of H , and p_Y as the marginal density of $Y = X + E$ (Gaussian or heavy-tailed component as required).

D.1 Proof of Theorem 4.1

Theorem 4.1 (Smooth shrinkage as a Bayes-motivated surrogate). *Let $y = x + e$, where $x \sim \mathcal{N}(0, \sigma_x^2)$ and $e \sim (1 - \alpha)\mathcal{N}(0, \sigma^2) + \alpha H$ with $\alpha \in [0, 1)$, and the heavy tailed density h associated with H satisfies the score and curvature conditions of Lemma D.3. Define the Wiener coefficient $\beta := \sigma_x^2 / (\sigma_x^2 + \sigma^2)$ and the (Bayesian) retention probability $\pi(y) := \Pr(e \sim \mathcal{N} \mid y)$.*

- (i) **Asymptotic Bayes structure.** *For every $\varepsilon > 0$ there exists an explicit threshold $y^* = y^*(\varepsilon, h, \sigma_x) \in (0, \infty)$ such that for all $|y| \geq y^*$ the Bayes optimal entrywise estimator admits the factorization*

$$\mathbb{E}[x \mid y] = \pi(y) \beta y + \rho(y), \quad |\rho(y)| \leq \varepsilon. \quad (11)$$

Combined with the entrywise MSE upper bound of Proposition 3.5, this controls the spectral perturbation $\mathbb{E}[|\sigma_1(\varphi_\tau(\tilde{G})) - \sigma_1(G)|^2]$.

- (ii) **Unique closed form surrogate.** *Among continuous functions $\hat{\pi} : [0, \infty) \rightarrow (0, 1]$ satisfying $\hat{\pi}(y) \rightarrow 0$ as $y \rightarrow \infty$ (re-descending), $\hat{\pi}(y_1 + y_2) = \hat{\pi}(y_1) \hat{\pi}(y_2)$ (multiplicative), and $\hat{\pi}(0) = 1$ (unit at origin), the unique one parameter family is $\hat{\pi}(y) = e^{-y/\tau}$ for some $\tau > 0$. Replacing π in Equation (11) with the even extension $y \mapsto e^{-|y|/\tau}$ yields the smooth shrinkage operator*

$$\varphi_\tau(y) := \beta e^{-|y|/\tau} y. \quad (12)$$

We separate the detailed proof of Theorem 4.1 into two parts:

Proof of Part (i): the Bayes-optimal estimator

The proof of part (i) combines two short propositions with a posterior collapse lemma. Here, we let $Z \in \{\mathcal{N}, H\}$ denote the latent mixture indicator, with $\Pr(Z = \mathcal{N}) = 1 - \alpha$. In Proposition D.1, we expand the conditional expectation using the latent indicator variable, and in Proposition D.2, we present the result of the conditional expectation using a conjugate prior.

Proposition D.1 (Mixture decomposition of the posterior mean). *Conditioning on the latent indicator Z and applying the tower property, we have $\mathbb{E}[x \mid y] = \pi(y) \mathbb{E}[x \mid y, Z = \mathcal{N}] + (1 - \pi(y)) \mathbb{E}[x \mid y, Z = H]$.*

Proposition D.2 (Conjugate Gaussian component). *For $x \sim \mathcal{N}(0, \sigma_x^2)$ and $e \mid Z = \mathcal{N} \sim \mathcal{N}(0, \sigma^2)$ independent of x , the standard Gaussian conjugate calculation gives $\mathbb{E}[x \mid y, Z = \mathcal{N}] = \beta y$ with $\beta = \sigma_x^2 / (\sigma_x^2 + \sigma^2)$.*

Lemma D.3 (Posterior collapse of the heavy tailed component). *Let $x \sim \mathcal{N}(0, \sigma_x^2)$ and let $e \sim H$ be independent of x , where the density h is strictly positive and lies in $C^2(\mathbb{R})$. Suppose there exist constants $C_1, C_2, T_0 > 0$ such that for all $|t| \geq T_0$,*

$$\left| \frac{d}{dt} \log h(t) \right| \leq \frac{C_1}{|t|}, \quad \left| \frac{d^2}{dt^2} \log h(t) \right| \leq \frac{C_2}{t^2}. \quad (25)$$

Then there exist explicit constants $\tilde{C} = 3C_1$ and $y_1 = y_1(C_1, C_2, T_0, h, \sigma_x) < \infty$ such that $|\mathbb{E}[x \mid y, Z = H]| \leq \frac{\tilde{C} \sigma_x^2}{|y|}$ for all $|y| \geq y_1$. In particular, for any $\varepsilon > 0$ and $|y| \geq \max(y_1, \tilde{C} \sigma_x^2 / \varepsilon)$, $|\mathbb{E}[x \mid y, Z = H]| \leq \varepsilon$.

We want to note that the conditions in Equation (25) from the above lemma are mild. The Student t_ν family for any $\nu > 0$ (including the Cauchy case $\nu = 1$) satisfies them with $C_1 = C_2 = \nu + 1$ and $T_0 = \sqrt{\nu}$, and symmetric stable laws satisfy them analogously [43]. The intuition for the above lemma is that for observation $|y| \gg \sigma_x$, the heavy tailed likelihood $h(y - x)$ is nearly flat over the effective support of the prior, so the posterior reverts toward $\mathcal{N}(0, \sigma_x^2)$ and concentrates near the origin. This is the classical outlier rejection phenomenon for heavy tailed likelihoods studied by O’Hagan [44] and Pericchi and Smith [45]. For completeness, we provide complete proof of Lemma D.3 in Section D.2.

Complete Proof of Part (i). Combining Proposition D.1, Proposition D.2, and Lemma D.3, for $|y| \geq y^* := \max(y_1, \tilde{C}\sigma_x^2/\varepsilon)$ we obtain $\mathbb{E}[x | y] = \pi(y)\beta y + \rho(y)$, where $\rho(y) = (1 - \pi(y))\mathbb{E}[x | y, Z = H]$. Since $1 - \pi(y) \in [0, 1]$, the lemma gives $|\rho(y)| \leq |\mathbb{E}[x | y, Z = H]| \leq \varepsilon$. The bound is uniform in the contamination parameters (α, σ) . \square

Proof of Part (ii): the Unique Closed Form Surrogate By Bayes’ rule, the exact retention probability $\pi(y) = \Pr[e \sim \mathcal{N} | y]$ is

$$\pi(y) = \frac{\Pr[y|e \sim \mathcal{N}] \cdot \Pr[e \sim \mathcal{N}]}{\Pr[y|e \sim \mathcal{N}] \cdot \Pr[e \sim \mathcal{N}] + \Pr[y|e \sim H] \cdot \Pr[e \sim H]} \quad (26)$$

$$= \left[1 + \frac{\alpha}{1-\alpha} \cdot \frac{f_{Y|Z=H}(y)}{f_{Y|Z=\mathcal{N}}(y)} \right]^{-1}, \quad (27)$$

with $f_{Y|Z=\mathcal{N}} = \mathcal{N}(0, \sigma_x^2 + \sigma^2)$ and $f_{Y|Z=H} = \phi_{\sigma_x} * h$. The right hand side admits no closed form, depends on (α, σ, h) , and decays faster than any exponential in $|y|$ because $f_{Y|Z=\mathcal{N}}$ is Gaussian while $f_{Y|Z=H}$ has heavy tails. We therefore replace π by a closed form surrogate $\hat{\pi}$ obeying the three axioms stated in Theorem 4.1.

Justification of the axioms. *Redescending.* The surrogate $\hat{\pi}$ must satisfy $\hat{\pi}(y) \rightarrow 0$ as $|y| \rightarrow \infty$, mirroring π itself: in Equation (27), $f_{Y|Z=H}(y)/f_{Y|Z=\mathcal{N}}(y) \rightarrow \infty$, so $\pi(y) \rightarrow 0$.

Multiplicative accumulation. We require that evidence of contamination accumulate at a constant rate per unit of magnitude, independently of the magnitude already accumulated. Equivalently, $\hat{\pi}(y_1 + y_2) = \hat{\pi}(y_1)\hat{\pi}(y_2)$.

Unit at origin. An observation of zero magnitude carries no evidence of contamination and is treated as Gaussian, i.e., $\hat{\pi}(0) = 1$.

Complete Proof of Part (ii). The multiplicative axiom is the Cauchy exponential functional equation on $[0, \infty)$. Under continuity, its only solutions $\hat{\pi} : [0, \infty) \rightarrow (0, 1]$ are the exponentials $\hat{\pi}(y) = e^{-cy}$ for some $c \geq 0$. The redescending axiom forces $c > 0$. Writing $c = 1/\tau$ for $\tau > 0$ and extending evenly to \mathbb{R} via $y \mapsto |y|$ yields $\hat{\pi}(y) = e^{-|y|/\tau}$. Substituting into Equation (11) gives the smooth shrinkage operator $\varphi_\tau(y) = \beta e^{-|y|/\tau} y$, which completes the proof of Theorem 4.1. \square

D.2 Proof of Lemma D.3

Lemma D.3 (Posterior collapse of the heavy tailed component). *Let $x \sim \mathcal{N}(0, \sigma_x^2)$ and let $e \sim H$ be independent of x , where the density h is strictly positive and lies in $C^2(\mathbb{R})$. Suppose there exist constants $C_1, C_2, T_0 > 0$ such that for all $|t| \geq T_0$,*

$$\left| \frac{d}{dt} \log h(t) \right| \leq \frac{C_1}{|t|}, \quad \left| \frac{d^2}{dt^2} \log h(t) \right| \leq \frac{C_2}{t^2}. \quad (25)$$

Then there exist explicit constants $\tilde{C} = 3C_1$ and $y_1 = y_1(C_1, C_2, T_0, h, \sigma_x) < \infty$ such that $|\mathbb{E}[x | y, Z = H]| \leq \frac{\tilde{C}\sigma_x^2}{|y|}$ for all $|y| \geq y_1$. In particular, for any $\varepsilon > 0$ and $|y| \geq \max(y_1, \tilde{C}\sigma_x^2/\varepsilon)$, $|\mathbb{E}[x | y, Z = H]| \leq \varepsilon$.

Proof. Here we give a non-asymptotic proof for the posterior collapse, under the assumption of score and curvature condition in Equation (25). We write $X \sim \mathcal{N}(0, \sigma_x^2)$, $E \sim H$ independent of X , $Y = X + E$, marginal $p_Y(y) = \int \phi_{\sigma_x}(x) h(y-x) dx$, and posterior mean $m(y) := \mathbb{E}[X | Y = y]$. We set $\psi(u) := -(\log h)'(u) = -h'(u)/h(u)$; by Equation (25), $|\psi(u)| \leq C_1/|u|$ for $|u| \geq T_0$.

Tweedie-type identity. Since $m(y) = E[X|Y = y] = \int x \frac{p_{X,Y}(x,y)}{p_Y(y)} dx$, and $p_{X,Y}(x, y) = p_X(x)p_{Y|X}(y|x)$ we have

$$\begin{aligned} m(y) p_Y(y) &= \int x \phi_{\sigma_x}(x) h(y-x) dx \\ &\stackrel{(a)}{=} -\sigma_x^2 \int \phi'_{\sigma_x}(x) h(y-x) dx \\ &\stackrel{(b)}{=} -\sigma_x^2 \int \phi_{\sigma_x}(x) h'(y-x) \cdot (-1) dx \\ &\stackrel{(c)}{=} \sigma_x^2 \int \phi_{\sigma_x}(x) \psi(y-x) h(y-x) dx, \\ &\stackrel{(d)}{=} \sigma_x^2 \mathbb{E}[\psi(Y-X) | Y = y] p_Y(y). \end{aligned} \tag{28}$$

where (a) uses $x \phi_{\sigma_x}(x) = -\sigma_x^2 \phi'_{\sigma_x}(x)$, (b) uses integration by parts (boundary terms vanish since $\phi_{\sigma_x} \rightarrow 0$ super-exponentially and h is bounded), (c) uses $h'(u) = -\psi(u)h(u)$, and (d) uses the definition of conditional expectation of $\psi(Y-X)$.

Global bound on ψ . We claim $\|\psi\|_\infty \leq M := \max(\sup_{|u| \leq T_0} |\psi(u)|, (C_1 + C_2)/T_0) < \infty$. On $[-T_0, T_0]$, ψ is continuous (since $h \in C^1$ and $h > 0$) hence bounded. For $|u| \geq T_0$, $|\psi'(u)| = |(\log h)''(u)| \leq C_2/u^2$ by Equation (25), so $|\psi(u)| \leq |\psi(T_0)| + \int_{T_0}^{|u|} |\psi'(s)| ds \leq C_1/T_0 + \int_{T_0}^\infty C_2/s^2 ds = (C_1 + C_2)/T_0$.

Bound $m(y)$ via event splitting. We create two event A and A^c that splits $Y - X$ into a good and bad region. In particular, fix $|y| \geq 2T_0$ and split on $A := \{|Y - X| > |y|/2\}$. On A , $|Y - X| \geq T_0$, and the score bound gives $|\psi(Y - X)| \leq C_1/|Y - X| \leq 2C_1/|y|$. On A^c , $|Y - X| \leq T_0$, the global bound gives $|\psi(Y - X)| \leq M$. Using the Tweedie-type identity Equation (28) we have

$$|m(y)| \leq \sigma_x^2 \left[\frac{2C_1}{|y|} \mathbb{P}(A | Y = y) + M \mathbb{P}(A^c | Y = y) \right] \leq \frac{2C_1 \sigma_x^2}{|y|} + M \sigma_x^2 \mathbb{P}(A^c | Y = y). \tag{29}$$

Bound $\mathbb{P}(A^c | Y = y)$. WLOG, we assume $y > 0$ (the case $y < 0$ is symmetric). Then $A^c = \{X \in [y/2, 3y/2]\}$ and $\mathbb{P}(A^c | Y = y) = \int_{y/2}^{3y/2} \phi_{\sigma_x}(x) h(y-x) dx / p_Y(y)$. We want to show $\mathbb{P}(A^c | Y = y)$ will become exponentially small when y closes to x . In particular, We bound the numerator and denominator using the power-law envelopes from Lemma D.4 below.

Numerator. On A^c , let $u := y - x$, we know $|u| \leq y/2$ and ϕ_{σ_x} is maximized at $x = y/2$: $\phi_{\sigma_x}(x) \leq \frac{1}{\sqrt{2\pi}\sigma_x} e^{-y^2/(8\sigma_x^2)}$. Setting $H_0 := \sup_{|u| \leq T_0} h(u) < \infty$ and using Lemma D.4 on $T_0 \leq |u| \leq y/2$, $\sup_{|u| \leq 2|y|} h(u) \leq \max(H_0, h(T_0))(2|y|/T_0)^{C_1} =: K_1(|y|)$, hence

$$\int_{y/2}^{3y/2} \phi_{\sigma_x}(x) h(y-x) dx \leq y \cdot \frac{e^{-y^2/(8\sigma_x^2)}}{\sqrt{2\pi}\sigma_x} \cdot K_1(y). \tag{30}$$

Denominator. To derive a lower bound for p_Y on \mathbb{R} , we first restrict p_Y to $|x| \leq 1$. Then $\phi_{\sigma_x}(x) \geq \frac{1}{\sqrt{2\pi}\sigma_x} e^{-1/(2\sigma_x^2)}$. For $|y| \geq T_0 + 1$, Lemma D.4 gives the lower envelope

$h(y - x) \geq h(T_0) (T_0/(|y| + 1))^{C_1}$, hence

$$p_Y(y) \geq 2 \cdot \frac{e^{-1/(2\sigma_x^2)}}{\sqrt{2\pi\sigma_x}} \cdot h(T_0) (T_0/(|y| + 1))^{C_1}. \quad (31)$$

Ratio. Dividing Equation (30) by Equation (31), the $1/(\sqrt{2\pi}\sigma_x)$ factors cancel:

$$\mathbb{P}(A^c \mid Y = y) \leq \underbrace{\frac{|y|}{2} \cdot \frac{K_1(|y|)}{h(T_0)} \cdot \left(\frac{|y|+1}{T_0}\right)^{C_1} \cdot e^{-y^2/(8\sigma_x^2)+1/(2\sigma_x^2)}}_{=:R(y)}. \quad (32)$$

$R(y)$ is the product of an at-most-polynomial factor (degree $C_1 + \max(1, C_1)$ in $|y|$) and the Gaussian factor $e^{-y^2/(8\sigma_x^2)}$, hence decays super-exponentially as $|y| \rightarrow \infty$.

Put every together. Substituting Equation (32) into Equation (29), $|m(y)| \leq 2C_1\sigma_x^2/|y| + M\sigma_x^2 R(y)$. Define $y_1 \geq 2T_0$ as the smallest value such that $M R(y) \leq C_1/|y|$ for all $|y| \geq y_1$. For $|y| \geq y_1$, $|m(y)| \leq 2C_1\sigma_x^2/|y| + \sigma_x^2 C_1/|y| = 3C_1\sigma_x^2/|y|$, proving Lemma D.3 with $\tilde{C} = 3C_1$. The ε -form follows by taking $|y| \geq \max(y_1, \tilde{C}\sigma_x^2/\varepsilon)$. \square

Lemma D.4 (Power-law envelope from score control). *Under the score condition $|(\log h)'(t)| \leq C_1/|t|$ on $|t| \geq T_0$, for every $|t| \geq T_0$, $h(T_0) (T_0/|t|)^{C_1} \leq h(t) \leq h(T_0) (|t|/T_0)^{C_1}$.*

Proof. Since $h(s)$ is symmetric, Without loss of generality, for $t \geq T_0$, $\log h(t) - \log h(T_0) = \int_{T_0}^t (\log h)'(s) ds$, so $|\log h(t) - \log h(T_0)| \leq C_1 \int_{T_0}^t ds/s = C_1 \log(t/T_0)$. Taking the exponentiation on both sides yields the two-sided bound. \square

E Proofs for Section 5

This section proves the four theorems in Section 5. We start the convergence proof with an entry-wise property on the gradient matrix that can be proved under a known Cauchy distribution. The same scalar property are used twice: first for post-clipping of one noisy gradient, and then for pre-clipped Muon. Throughout the appendix, $\mathbb{E}_k[\cdot]$ denotes conditional expectation over minibatch ξ_k given filtration $\mathcal{F}_{k-1} = \sigma(\xi_1, \dots, \xi_{k-1})$. $G \in \mathbb{R}^{m \times n}$ is the true gradient matrix and $g := (G)_{ij}$ is the gradient entry inside the true gradient matrix G .

The relative-bias principle for matrix scalars For an entry-wise pre-processing map φ , define the scalar processed mean

$$m_\varphi(g) := \mathbb{E}_\xi \varphi(g + \xi), \quad \xi \sim (1 - \alpha)N(0, \sigma^2) + \alpha \text{Cauchy}(0, \gamma). \quad (33)$$

For a matrix G , $m_\varphi(G)$ means that Equation (33) is applied entry by entry. We isolate the central scalar estimate as a named property that all four convergence theorems will rely on.

Definition E.1 (Relative-Bias Property). A coordinate-wise map $\varphi : \mathbb{R} \rightarrow \mathbb{R}$ satisfies the *relative-bias property* with constant $\rho \in [0, 1)$ on $[-B, B]$ under the noise model Equation (33) if, for every $|g| \leq B$,

$$|m_\varphi(g) - g| \leq \rho |g|. \quad (34)$$

Equation (34) is not an unbiasedness statement: it says that the processed conditional mean is a *multiplicative* perturbation of the clean signal. This is a stronger result than a uniform additive-bias bound for optimization, because the bias vanishes whenever the true gradient entry is zero. In general,

$$m_\varphi(g) = \mathbb{E} \varphi(g + \xi) \neq \varphi(g) \quad \text{and} \quad m_\varphi(g) \neq g.$$

Lemmas E.4 and E.8 establish this relative-bias property for C_τ and S_c respectively, with explicit constants ρ_τ and ρ_c that depend on the threshold and the noise scales. Next, we show how we use the relative bias alignment result to prove the convergence result for both post-clipping and pre-clipping.

Relative bias alignment in *post-clipping* For the post-clipped update Equation (14), define

$$Y_k^\varphi := \varphi(G_k + \Xi_k), \quad M_{k,\text{post}}^\varphi := \mathbb{E}_k Y_k^\varphi = m_\varphi(G_k). \quad (35)$$

If Equation (34) holds entrywise for all k , then

$$\|M_{k,\text{post}}^\varphi - G_k\|_F \leq \rho \|G_k\|_F. \quad (36)$$

Consequently,

$$\begin{aligned} \langle G_k, M_{k,\text{post}}^\varphi \rangle &= \|G_k\|_F^2 + \langle G_k, M_{k,\text{post}}^\varphi - G_k \rangle \\ &\geq \|G_k\|_F^2 - \|G_k\|_F \|M_{k,\text{post}}^\varphi - G_k\|_F \\ &\geq (1 - \rho) \|G_k\|_F^2. \end{aligned} \quad (37)$$

This is the post-clipping use of the relative-bias principle: it converts a biased processed update into a direction that remains positively aligned with the true gradient, provided $\rho < 1$.

Relative bias absorption in *pre-clipping* For pre-clipping, the processed mini-batch mean is

$$\bar{G}_k^\varphi = \frac{1}{N} \sum_{\ell=1}^N \varphi(G_k + \Xi_k^{(\ell)}), \quad M_{k,\text{pre}}^\varphi := \mathbb{E}_k \bar{G}_k^\varphi = m_\varphi(G_k). \quad (38)$$

The exact decomposition is

$$\bar{G}_k^\varphi - G_k = \underbrace{(\bar{G}_k^\varphi - M_{k,\text{pre}}^\varphi)}_{\text{zero-mean processed sampling fluctuation}} + \underbrace{(M_{k,\text{pre}}^\varphi - G_k)}_{\text{deterministic conditional bias}}. \quad (39)$$

The first term is controlled by a variance estimate for $\varphi(g + \xi)$ and by independence across the sample index. The second term is deterministic conditional on X_k . If Equation (34) holds for all k ,

$$\|M_{k,\text{pre}}^\varphi - G_k\|_* \leq \sqrt{r} \|M_{k,\text{pre}}^\varphi - G_k\|_F \leq \sqrt{r}\rho \|G_k\|_F \leq \sqrt{r}\rho \|G_k\|_*. \quad (40)$$

When this is inserted into the matrix-sign descent lemma, it appears on the same side as the stationarity measure $\|G_k\|_*$ and can be moved to the left as long as $2\sqrt{r}\rho < 1$. This is the pre-clipped Muon use of the same principle. The difference between Equation (37) and Equation (40) is purely algorithmic: post-clipping needs alignment of the processed update with G_k , while Muon needs a nuclear-norm control of the error in the matrix-sign direction.

Organization. We first present preliminary Lemmas in Section E.1. In Section E.2 and Section E.3, we prove both hard clipping operator $C_\tau(x)$ and smooth shrinkage $S_c(x)$ satisfies the Relative-Bias property in Definition E.1. In Section E.5, we apply this property to the descent lemma given by L -smoothness and prove the convergence result of Theorem 5.4 and Theorem 5.5. Similarly, we use the same trick to prove Theorem 5.6 and Theorem 5.7 in Section E.6.

E.1 Elementary Scalar Inequalities

Lemma E.2 (Gaussian and Cauchy tails). *Let $Z \sim N(0, \sigma^2)$ and $H \sim \text{Cauchy}(0, \gamma)$. For $t \geq 0$,*

$$\mathbb{P}(|Z| \geq t) \leq 2 \exp\left(-\frac{t^2}{2\sigma^2}\right), \quad (41)$$

with the convention that this probability is zero when $\sigma = 0 < t$. For $a > 0$,

$$\mathbb{P}(H > a) = \mathbb{P}(H < -a) = \frac{1}{\pi} \arctan\left(\frac{\gamma}{a}\right) \leq \frac{\gamma}{\pi a}. \quad (42)$$

Moreover,

$$\mathbb{E} \min\{H^2, a^2\} \leq \frac{4\gamma a}{\pi}, \quad (43)$$

and the one-sided version obeys

$$\int_0^\infty \min\{h^2, a^2\} \frac{\gamma}{\pi(\gamma^2 + h^2)} dh \leq \frac{2\gamma a}{\pi}. \quad (44)$$

Proof. The Gaussian bound is the standard Chernoff tail bound. For the Cauchy tail, integrate the density:

$$\mathbb{P}(H > a) = \int_a^\infty \frac{\gamma}{\pi(\gamma^2 + h^2)} dh = \frac{1}{\pi} \arctan\left(\frac{\gamma}{a}\right) \leq \frac{\gamma}{\pi a},$$

where the last step uses $\arctan x \leq x$ for $x \geq 0$. For the one-sided truncation bound, split the integral at a :

$$\int_0^a h^2 \frac{\gamma}{\pi(\gamma^2 + h^2)} dh \leq \int_0^a \frac{\gamma}{\pi} dh = \frac{\gamma a}{\pi},$$

and

$$\int_a^\infty a^2 \frac{\gamma}{\pi(\gamma^2 + h^2)} dh \leq a^2 \int_a^\infty \frac{\gamma}{\pi h^2} dh = \frac{\gamma a}{\pi}.$$

Adding these two estimates proves Equation (44); symmetry gives Equation (43). \square

Lemma E.3 (A logarithmic threshold device). *Let $a \geq 0$ and $s \geq 1$. If*

$$x \geq 2sa \log(e + 2sa),$$

then

$$\frac{a \log(e + x)}{x} \leq \frac{1}{s}.$$

Proof. If $a = 0$, the claim is immediate. Suppose $a > 0$ and set $A := 2sa$. The function $x/\log(e + x)$ is increasing on $(0, \infty)$ because

$$\frac{d}{dx} \frac{x}{\log(e + x)} = \frac{\log(e + x) - x/(e + x)}{\log^2(e + x)} > 0.$$

Therefore it is enough to verify the claim at $x_0 = A \log(e + A)$. Since

$$e + x_0 = e + A \log(e + A) \leq (e + A)^2,$$

we have $\log(e + x_0) \leq 2 \log(e + A)$. Hence

$$x_0 = A \log(e + A) \geq \frac{A}{2} \log(e + x_0) = sa \log(e + x_0),$$

which is the desired inequality at x_0 . \square

E.2 Proofs of Scalar Relative bias and Variance under C_τ

Recall $C_\tau(x) = \text{sign}(x) \min\{|x|, \tau\}$.

Lemma E.4 (Relative bias of hard clipping). *Let $|g| \leq B < \tau$, and let $\xi_0 \sim (1 - \alpha)N(0, \sigma_0^2) + \alpha \text{Cauchy}(0, \gamma_0)$ with $0 \leq \sigma_0 \leq \sigma$ and $0 < \gamma_0 \leq \gamma$. Then*

$$|\mathbb{E}C_\tau(g + \xi_0) - g| \leq \rho_\tau |g|, \quad (45)$$

where

$$\rho_\tau := 2(1 - \alpha) \bar{\Phi} \left(\frac{\tau - B}{\sigma} \right) + \frac{\alpha \gamma}{\pi} \left(\frac{1}{\tau - B} + \frac{1}{\tau + B} \right), \quad (46)$$

$\bar{\Phi}(t) := \mathbb{P}(N(0, 1) \geq t)$, and the Gaussian term is interpreted as zero when $\sigma = 0$.

Proof. We first prove the claim for a generic symmetric scalar noise W with a continuous density. Define

$$m_W(s) := \mathbb{E}C_\tau(s + W).$$

Because C_τ is odd and W is symmetric, $m_W(0) = 0$. The map C_τ is Lipschitz and is differentiable except at $\pm\tau$, with derivative $1\{|x| < \tau\}$ at differentiability points. Differentiating under the integral gives

$$m'_W(s) = \mathbb{P}(|s + W| < \tau).$$

Thus

$$m_W(g) - g = \int_0^g (m'_W(s) - 1) ds,$$

and hence

$$|m_W(g) - g| \leq |g| \sup_{|s| \leq B} \mathbb{P}(|s + W| \geq \tau).$$

For $W = Z \sim N(0, \sigma_0^2)$, if $|s| \leq B$ and $|s + Z| \geq \tau$, then $|Z| \geq \tau - B$, hence $\mathbb{P}(|s + Z| \geq \tau) \leq \mathbb{P}(|Z| \geq \tau - B)$. When $\sigma_0 > 0$ this is at most $2\bar{\Phi}((\tau - B)/\sigma_0)$ by the standard Gaussian tail bound; when $\sigma_0 = 0$, $Z \equiv 0$ and the probability is exactly zero, since $\tau > B$. Combining

the two cases under the convention that $\bar{\Phi}((\tau - B)/0) := 0$ (consistent with Equation (41)) and using monotonicity of $\bar{\Phi}$,

$$|m_Z(g) - g| \leq 2\bar{\Phi}\left(\frac{\tau - B}{\sigma_0}\right) |g| \leq 2\bar{\Phi}\left(\frac{\tau - B}{\sigma}\right) |g|.$$

For $W = H \sim \text{Cauchy}(0, \gamma_0)$, Equation (42) gives, uniformly over $|s| \leq B$,

$$\begin{aligned} \mathbb{P}(|s + H| \geq \tau) &= \mathbb{P}(H \geq \tau - s) + \mathbb{P}(H \leq -\tau - s) \\ &\leq \frac{\gamma_0}{\pi} \left(\frac{1}{\tau - s} + \frac{1}{\tau + s} \right) \leq \frac{\gamma_0}{\pi} \left(\frac{1}{\tau - B} + \frac{1}{\tau + B} \right) \leq \frac{\gamma}{\pi} \left(\frac{1}{\tau - B} + \frac{1}{\tau + B} \right), \end{aligned}$$

where the supremum over $|s| \leq B$ is achieved at the endpoints $s = \pm B$. Taking the mixture of the Gaussian and Cauchy bounds proves Equation (45). \square

Lemma E.5 (Variance of hard clipping). *Let $|g| \leq B < \tau$, let $\xi_0 \sim (1 - \alpha)N(0, \sigma_0^2) + \alpha\text{Cauchy}(0, \gamma_0)$ with $0 \leq \sigma_0 \leq \sigma$ and $0 < \gamma_0 \leq \gamma$. Then*

$$\text{Var}(C_\tau(g + \xi_0)) \leq v_\tau, \quad v_\tau := (1 - \alpha)\sigma^2 + \frac{4\alpha\gamma\tau}{\pi}. \quad (47)$$

Proof. For any random variable Y and deterministic number a , $\text{Var}(Y) \leq \mathbb{E}(Y - a)^2$. Here we choose the center $a = g$. This is natural for hard clipping because $C_\tau(g) = g$ whenever $|g| \leq B < \tau$.

For the Gaussian branch, C_τ is 1-Lipschitz, so

$$|C_\tau(g + Z) - g| = |C_\tau(g + Z) - C_\tau(g)| \leq |Z|.$$

Thus the Gaussian contribution is at most $\mathbb{E}Z^2 = \sigma_0^2 \leq \sigma^2$.

For the Cauchy branch, use the positive and negative halves separately. If $h \geq 0$, then moving from g to $g + h$ can increase the clipped value by at most $\tau - g$, so

$$|C_\tau(g + h) - g| = \min\{h, \tau - g\}.$$

If $h \leq 0$, then moving from g to $g + h$ can decrease the clipped value by at most $\tau + g$, so

$$|C_\tau(g + h) - g| = \min\{|h|, \tau + g\}.$$

Applying the one-sided truncation bound Equation (44) to the two halves gives

$$\mathbb{E}|C_\tau(g + H) - g|^2 \leq \frac{2\gamma_0(\tau - g)}{\pi} + \frac{2\gamma_0(\tau + g)}{\pi} = \frac{4\gamma_0\tau}{\pi} \leq \frac{4\gamma\tau}{\pi}.$$

Mixing the two branches proves the lemma. \square

E.3 Proofs of Scalar Relative bias and Variance under S_c

Recall $S_c(x) = xe^{-|x|/c}$.

Lemma E.6 (Elementary properties of smooth shrinkage). *The map S_c is odd, 1-Lipschitz, and satisfies $|S_c(x)| \leq c/e$ for all x . Its derivative is*

$$S'_c(x) = e^{-|x|/c} \left(1 - \frac{|x|}{c} \right),$$

and S'_c is $2/c$ -Lipschitz.

Proof. Oddness is immediate. For $x \neq 0$, the displayed derivative follows by differentiating on the two half-lines; the same formula gives the derivative at 0. With $t = |x|/c$,

$$|S'_c(x)| = e^{-t}|1-t| \leq 1,$$

so S_c is 1-Lipschitz. Also

$$|S_c(x)| = |x|e^{-|x|/c} = cte^{-t} \leq c/e.$$

Finally, write $S'_c(x) = h(|x|/c)$ with $h(t) = e^{-t}(1-t)$. Since $|h'(t)| = e^{-t}|t-2| \leq 2$ for $t \geq 0$,

$$|S'_c(x) - S'_c(y)| \leq \frac{2}{c} ||x| - |y|| \leq \frac{2}{c}|x - y|.$$

□

Lemma E.7 (Derivative deficits for smooth shrinkage). *Let $Z \sim N(0, \sigma^2)$ and $H \sim \text{Cauchy}(0, \gamma)$. Define*

$$\mu_c := \mathbb{E}S'_c(Z), \quad \kappa_c := \mathbb{E}S'_c(H).$$

Then

$$1 - \mu_c \leq \sqrt{\frac{8}{\pi}} \frac{\sigma}{c}, \quad 1 - \kappa_c \leq \frac{8\gamma}{\pi c} \log\left(e + \frac{c}{\gamma}\right). \quad (48)$$

Proof. For $t \geq 0$, the elementary inequality

$$1 - e^{-t}(1-t) \leq 2t$$

holds. Therefore

$$1 - \mu_c = \mathbb{E}\left[1 - e^{-|Z|/c} \left(1 - \frac{|Z|}{c}\right)\right] \leq \frac{2}{c} \mathbb{E}|Z| = \sqrt{\frac{8}{\pi}} \frac{\sigma}{c}.$$

For the Cauchy branch, symmetry gives

$$1 - \kappa_c = \frac{2\gamma}{\pi} \int_0^\infty \frac{1 - e^{-u/c}(1 - u/c)}{\gamma^2 + u^2} du.$$

Split the integral into $[0, c]$ and $[c, \infty)$. On $[0, c]$, use $1 - e^{-u/c}(1 - u/c) \leq 2u/c$. On $[c, \infty)$, use the crude bound $1 - e^{-u/c}(1 - u/c) \leq 2$. Then

$$\begin{aligned} 1 - \kappa_c &\leq \frac{2\gamma}{\pi} \left[\frac{2}{c} \int_0^c \frac{u}{\gamma^2 + u^2} du + 2 \int_c^\infty \frac{1}{\gamma^2 + u^2} du \right] \\ &\leq \frac{2\gamma}{\pi c} \log\left(1 + \frac{c^2}{\gamma^2}\right) + \frac{4\gamma}{\pi c}. \end{aligned}$$

Since $\log(1+x^2) \leq 2\log(e+x)$ and $1 \leq \log(e+x)$ for $x \geq 0$, this is at most $8\gamma(\pi c)^{-1} \log(e + c/\gamma)$. □

Lemma E.8 (Relative bias of smooth shrinkage). *For $|g| \leq B$, let $\xi_0 \sim (1-\alpha)N(0, \sigma_0^2) + \alpha\text{Cauchy}(0, \gamma_0)$ with $0 \leq \sigma_0 \leq \sigma$ and $0 < \gamma_0 \leq \gamma$. Then*

$$|\mathbb{E}S_c(g + \xi_0) - g| \leq \rho_c |g|, \quad (49)$$

where

$$\rho_c := \frac{B + \sqrt{8/\pi}(1-\alpha)\sigma}{c} + \frac{8\alpha\gamma}{\pi c} \log\left(e + \frac{c}{\gamma}\right). \quad (50)$$

Proof. Because S_c is odd and ξ is symmetric, $\mathbb{E}S_c(\xi) = 0$. Since S'_c is $2/c$ -Lipschitz, Taylor's theorem with Lipschitz derivative gives, for every x and g ,

$$|S_c(x+g) - S_c(x) - gS'_c(x)| \leq \frac{g^2}{c}.$$

Set $x = \xi_0$ and take expectations. Then

$$\begin{aligned} |\mathbb{E}S_c(g + \xi_0) - g| &= |\mathbb{E}[S_c(g + \xi_0)] - S_c(\xi_0)] - g| \\ &\leq |g| |\mathbb{E}S'_c(\xi_0) - 1| + \frac{g^2}{c}. \end{aligned}$$

The derivative deficit of the mixture is

$$1 - \mathbb{E}S'_c(\xi_0) = (1 - \alpha)(1 - \mu_c) + \alpha(1 - \kappa_c).$$

Using Lemma E.7, $g^2/c \leq (B/c)|g|$, and monotonicity in γ and σ proves the displayed bound. The term B/c in ρ_c arises from this Taylor remainder: unlike hard clipping, which exactly satisfies $C_\tau(g) = g$ for $|g| \leq B < \tau$ and contributes no remainder, smooth shrinkage is only *approximately* the identity near zero, with a quadratic deviation that the threshold c must absorb. \square

Lemma E.9 (Variance of smooth shrinkage). *For $|g| \leq B$, let $\xi_0 \sim (1 - \alpha)N(0, \sigma_0^2) + \alpha\text{Cauchy}(0, \gamma_0)$ with $0 \leq \sigma_0 \leq \sigma$ and $0 < \gamma_0 \leq \gamma$. Then*

$$\text{Var}(S_c(g + \xi_0)) \leq v_c, \quad v_c := (1 - \alpha)\sigma^2 + \frac{8\alpha\gamma c}{\pi e}. \quad (51)$$

Proof. Use $\text{Var}(Y) \leq \mathbb{E}(Y - a)^2$ with the deterministic center $a = S_c(g)$. By Lemma E.6, S_c is 1-Lipschitz and $|S_c| \leq c/e$, so

$$|S_c(g + \xi_0) - S_c(g)| \leq \min\{|\xi|, 2c/e\}.$$

The Gaussian contribution is at most $\mathbb{E}Z^2 = \sigma^2$. The Cauchy contribution is bounded by

$$\mathbb{E} \min\{H^2, (2c/e)^2\} \leq \frac{8\gamma_0 c}{\pi e} \leq \frac{8\gamma c}{\pi e}$$

from Equation (43). Mixing the two branches proves the variance bound. \square

E.4 Proofs of Clipping Threshold τ and c

Recall in Equation (46) and Equation (50)

$$\begin{aligned} \rho_\tau &= 2(1 - \alpha)\bar{\Phi}\left(\frac{\tau - B}{\sigma}\right) + \frac{\alpha\gamma}{\pi} \left(\frac{1}{\tau - B} + \frac{1}{\tau + B}\right), \\ \rho_c &= \frac{B + \sqrt{8/\pi}(1 - \alpha)\sigma}{c} + \frac{8\alpha\gamma}{\pi c} \log\left(e + \frac{c}{\gamma}\right). \end{aligned}$$

We now verify that the thresholds in the main theorems make the relative-bias constants small enough.

Lemma E.10 (Post-clipping thresholds). *The hard-clipping threshold*

$$\tau \geq B + \max\left\{\sigma\sqrt{2\log 8}, \frac{8\alpha\gamma}{\pi}\right\},$$

implies $\rho_\tau \leq 1/2$. The smooth-shrinkage threshold

$$c \geq \max\left\{4\left[B + \sqrt{\frac{8}{\pi}}(1 - \alpha)\sigma\right], \frac{64\alpha\gamma}{\pi} \log\left(e + \frac{64\alpha}{\pi}\right)\right\},$$

implies $\rho_c \leq 1/2$.

Proof. For hard clipping, $\tau \geq B + \sigma\sqrt{2\log 8}$ gives

$$2(1 - \alpha)\bar{\Phi}\left(\frac{\tau - B}{\sigma}\right) \leq 2 \exp\{-\log 8\} = \frac{1}{4},$$

and, since $\tau + B > \tau - B$,

$$\frac{\alpha\gamma}{\pi} \left(\frac{1}{\tau - B} + \frac{1}{\tau + B} \right) \leq \frac{2\alpha\gamma}{\pi(\tau - B)} \leq \frac{1}{4}.$$

Thus $\rho_\tau \leq 1/2$.

For smooth shrinkage, the first part of the maximum in c gives

$$\frac{B + \sqrt{8/\pi}(1 - \alpha)\sigma}{c} \leq \frac{1}{4}.$$

For the logarithmic term, apply Lemma E.3 to the second part of the maximum in c with

$$x = \frac{c}{\gamma}, \quad a = \frac{8\alpha}{\pi}, \quad s = 4.$$

The second lower bound in c is $x \geq 2sa \log(e + 2sa)$, so

$$\frac{8\alpha\gamma}{\pi c} \log\left(e + \frac{c}{\gamma}\right) = \frac{a \log(e + x)}{x} \leq \frac{1}{4}.$$

Hence $\rho_c \leq 1/2$. □

Lemma E.11 (Pre-clipped Muon thresholds). *The hard-clipping threshold*

$$\tau \geq B + \max\left\{\sigma\sqrt{2\log(16\sqrt{r})}, \frac{16\alpha\gamma\sqrt{r}}{\pi}\right\},$$

implies $\rho_\tau \leq 1/(4\sqrt{r})$. The smooth-shrinkage threshold

$$c \geq \max\left\{8\sqrt{r}\left[B + \sqrt{\frac{8}{\pi}}(1 - \alpha)\sigma\right], \frac{128\alpha\gamma\sqrt{r}}{\pi} \log\left(e + \frac{128\alpha\gamma\sqrt{r}}{\pi}\right)\right\},$$

implies $\rho_c \leq 1/(4\sqrt{r})$.

Proof. For hard clipping, the Gaussian term satisfies

$$2(1 - \alpha)\bar{\Phi}\left(\frac{\tau - B}{\sigma}\right) \leq 2 \exp\{-\log(16\sqrt{r})\} = \frac{1}{8\sqrt{r}}.$$

The Cauchy term satisfies

$$\frac{\alpha\gamma}{\pi} \left(\frac{1}{\tau - B} + \frac{1}{\tau + B} \right) \leq \frac{2\alpha\gamma}{\pi(\tau - B)} \leq \frac{1}{8\sqrt{r}}.$$

Therefore $\rho_\tau \leq 1/(4\sqrt{r})$.

For smooth shrinkage, the first lower bound in gives

$$\frac{B + \sqrt{8/\pi}(1 - \alpha)\sigma}{c} \leq \frac{1}{8\sqrt{r}}.$$

For the logarithmic term, apply Lemma E.3 with

$$x = \frac{c}{\gamma}, \quad a = \frac{8\alpha}{\pi}, \quad s = 8\sqrt{r}.$$

The second lower bound in c becomes $x \geq 2sa \log(e + 2sa)$, hence

$$\frac{8\alpha\gamma}{\pi c} \log\left(e + \frac{c}{\gamma}\right) \leq \frac{1}{8\sqrt{r}}.$$

Thus $\rho_c \leq 1/(4\sqrt{r})$. □

E.5 Proofs of Theorems 5.4 and 5.5

Lemma E.12 (Post-clipping descent with relative bias). *Assume Assumptions 5.1 to 5.3. Let φ be applied coordinatewise and suppose that, for every $|g| \leq B$, the relative-bias property Equation (34) holds with constant $\rho < 1$, and the post-processed update is uniformly entry-wise bounded:*

$$|m_\varphi(g) - g| \leq \rho|g|, \quad |\varphi(x)| \leq R_\varphi \quad \text{for all } x.$$

The constant R_φ is the entry-wise sup-norm of the processed update; for the two maps used in this paper, $R_\varphi = \tau$ for hard clipping C_τ and $R_\varphi = c/e$ for smooth shrinkage S_c (Lemma E.6).

Then the post-clipped update Equation (14) with $\eta = \sqrt{2\Delta/(LR_\varphi^2 dK)}$ satisfies

$$\frac{1}{K} \sum_{k=0}^{K-1} \mathbb{E} \|G_k\|_F^2 \leq \frac{R_\varphi}{1-\rho} \sqrt{\frac{2L\Delta d}{K}}. \quad (52)$$

Proof. Define the conditional processed mean

$$M_k^\varphi := \mathbb{E}_k \varphi(G_k + \Xi_k) = m_\varphi(G_k),$$

applied entry by entry. The relative-bias assumption (this follows from Lemma E.4 and Lemma E.8 for $C_\tau(x)$ and $S_c(x)$) gives

$$\|M_k^\varphi - G_k\|_F \leq \rho \|G_k\|_F.$$

Therefore

$$\begin{aligned} \langle G_k, M_k^\varphi \rangle &= \|G_k\|_F^2 + \langle G_k, M_k^\varphi - G_k \rangle \\ &\geq \|G_k\|_F^2 - \|G_k\|_F \|M_k^\varphi - G_k\|_F \\ &\geq (1-\rho) \|G_k\|_F^2. \end{aligned}$$

This is the alignment step: the processed mean is biased, but the bias is not large enough to destroy its positive inner product with the true gradient.

By L -smoothness,

$$F(X_{k+1}) \leq F(X_k) - \eta \langle G_k, \varphi(G_k + \Xi_k) \rangle + \frac{L\eta^2}{2} \|\varphi(G_k + \Xi_k)\|_F^2.$$

Taking conditional expectation on step k and using $\|\varphi(G_k + \Xi_k)\|_F^2 \leq R_\varphi^2 d$ gives

$$\mathbb{E}_k F(X_{k+1}) \leq F(X_k) - \eta(1-\rho) \|G_k\|_F^2 + \frac{L\eta^2 R_\varphi^2 d}{2}.$$

Summing over $k = 0, \dots, K-1$, using $F(X_K) \geq \inf_X F(X)$, and dividing by $K\eta(1-\rho)$,

$$\frac{1}{K} \sum_{k=0}^{K-1} \mathbb{E} \|G_k\|_F^2 \leq \frac{\Delta}{K\eta(1-\rho)} + \frac{L\eta R_\varphi^2 d}{2(1-\rho)}.$$

With $\eta = \sqrt{2\Delta/(LR_\varphi^2 dK)}$, the two deterministic terms balance and their sum equals the right-hand side of Equation (52). \square

Theorem 5.4 (Post-clipping with hard clipping). *Under Assumptions 5.1 to 5.3, choose τ such that $\tau \geq B + \max\{\sigma\sqrt{2\log 8}, \frac{8\alpha\gamma}{\pi}\}$. Executing the update rule Equation (14) with $\varphi = C_\tau$ and a step size of $\eta = \sqrt{2\Delta/(L\tau^2 dK)}$ for K iterations yields:*

$$\frac{1}{K} \sum_{k=0}^{K-1} \mathbb{E} \|G_k\|_F^2 \leq 2\tau \sqrt{\frac{2L\Delta d}{K}}. \quad (15)$$

Consequently, when $K \geq 8L\Delta d\tau^2/\varepsilon^4$, we guarantee $\frac{1}{K} \sum_{k=0}^{K-1} \mathbb{E} \|G_k\|_F \leq \varepsilon$.

Proof. By Lemma E.4, at any iteration k , for gradient noise ξ_k with $0 \leq \sigma_k \leq \sigma$ and $0 \leq \gamma_k \leq \gamma$, hard clipping has a uniform relative-bias coefficient ρ_τ . By Lemma E.10, the threshold assumed in the theorem gives $\rho_\tau \leq 1/2$. Also $|C_\tau(x)| \leq \tau$, so Lemma E.12 applies with $R_\varphi = \tau$ and $1/(1 - \rho_\tau) \leq 2$. This proves the displayed average squared-gradient bound. Finally, Jensen's inequality gives

$$\frac{1}{K} \sum_{k=0}^{K-1} \mathbb{E} \|G_k\|_F \leq \left(\frac{1}{K} \sum_{k=0}^{K-1} \mathbb{E} \|G_k\|_F^2 \right)^{1/2},$$

and the stated lower bound on K makes the right-hand side at most ε . \square

Theorem 5.5 (Post-clipping with smooth shrinkage). *Under Assumptions 5.1 to 5.3, choose $c \geq \max \left\{ 4 \left[B + \sqrt{\frac{8}{\pi}}(1 - \alpha)\sigma \right], \frac{64\alpha\gamma}{\pi} \log \left(e + \frac{64\alpha}{\pi} \right) \right\}$. Executing the update rule Equation (14) with $\varphi = S_c$ and a step size of $\eta = e\sqrt{2\Delta/(Lc^2dK)}$ for K iterations yields:*

$$\frac{1}{K} \sum_{k=0}^{K-1} \mathbb{E} \|G_k\|_F^2 \leq \frac{2c}{e} \sqrt{\frac{2L\Delta d}{K}}. \quad (16)$$

Consequently, when $K \geq 8L\Delta dc^2/(e^2\varepsilon^4)$, we guarantee $\frac{1}{K} \sum_{k=0}^{K-1} \mathbb{E} \|G_k\|_F \leq \varepsilon$.

Proof. By Lemma E.8, at any iteration k , for gradient noise ξ_k with $0 \leq \sigma_k \leq \sigma$ and $0 \leq \gamma_k \leq \gamma$, smooth shrinkage has a uniform relative-bias coefficient ρ_c . By Lemma E.10, the threshold choice c in the theorem gives $\rho_c \leq 1/2$. Also $|S_c(x)| \leq c/e$ by Lemma E.6. Applying Lemma E.12 with $R_\varphi = c/e$ gives the displayed average squared-gradient bound. Jensen's inequality gives the stated K condition for the average gradient norm. \square

E.6 Proofs of Theorems 5.6 and 5.7

Lemma E.13 (Matrix-sign descent). *Let \bar{G}_k be any matrix and set $E_k := \bar{G}_k - G_k$. For*

$$X_{k+1} = X_k - \eta \operatorname{msign}(\bar{G}_k),$$

one has

$$F(X_{k+1}) \leq F(X_k) - \eta \|G_k\|_* + 2\eta \|E_k\|_* + \frac{L\eta^2 r}{2}. \quad (53)$$

Proof. Let $U_k := \operatorname{msign}(\bar{G}_k)$. By L -smoothness,

$$F(X_{k+1}) \leq F(X_k) - \eta \langle G_k, U_k \rangle + \frac{L\eta^2}{2} \|U_k\|_F^2.$$

The matrix U_k has at most r nonzero singular values, each equal to one, so $\|U_k\|_F^2 \leq r$ and $\|U_k\|_{\text{op}} \leq 1$. Moreover, by the definition of the matrix sign,

$$\langle \bar{G}_k, U_k \rangle = \|\bar{G}_k\|_*.$$

Using $E_k = \bar{G}_k - G_k$,

$$\begin{aligned} \langle G_k, U_k \rangle &= \langle \bar{G}_k, U_k \rangle - \langle E_k, U_k \rangle \\ &\geq \|\bar{G}_k\|_* - \|E_k\|_* \|U_k\|_{\text{op}} \\ &\geq \|\bar{G}_k\|_* - \|E_k\|_*. \end{aligned}$$

The reverse triangle inequality gives $\|\bar{G}_k\|_* \geq \|G_k\|_* - \|E_k\|_*$. Hence

$$\langle G_k, U_k \rangle \geq \|G_k\|_* - 2\|E_k\|_*.$$

Substituting this into the smoothness inequality proves the lemma. \square

Lemma E.14 (Pre-clipped Muon under relative bias and finite processed variance). *Assume Assumptions 5.1 to 5.3. Suppose φ satisfies, for all $|g| \leq B$, we can a uniform ρ such that*

$$|m_\varphi(g) - g| \leq \rho|g|, \quad \text{Var}(\varphi(g + \xi)) \leq v.$$

Run Equation (17) with $\eta = \sqrt{2\Delta/(LrT)}$. If $2\sqrt{r}\rho < 1$, then

$$\frac{1}{T} \sum_{k=0}^{T-1} \mathbb{E} \|G_k\|_* \leq \frac{\sqrt{2Lr\Delta/T} + 2Dr^{3/2}\sqrt{v/N}}{1 - 2\sqrt{r}\rho}. \quad (54)$$

Proof. Let $M_k^\varphi := \mathbb{E}_k \bar{G}_k^\varphi = m_\varphi(G_k)$. Use the exact decomposition

$$\bar{G}_k^\varphi - G_k = (\bar{G}_k^\varphi - M_k^\varphi) + (M_k^\varphi - G_k).$$

We bound the two terms separately.

First consider the zero-mean stochastic part. Each entry of $\bar{G}_k^\varphi - M_k^\varphi$ is an average of N independent processed samples, so its conditional variance is at most v/N . Hence

$$\begin{aligned} \mathbb{E}_k \|\bar{G}_k^\varphi - M_k^\varphi\|_* &\leq \sqrt{r} \mathbb{E}_k \|\bar{G}_k^\varphi - M_k^\varphi\|_F \\ &\leq \sqrt{r} \left(\mathbb{E}_k \|\bar{G}_k^\varphi - M_k^\varphi\|_F^2 \right)^{1/2} \\ &\leq \sqrt{r} \sqrt{d \frac{v}{N}}. \end{aligned}$$

Since $d = mn = rq$ and $D = \sqrt{q/r}$, we have $\sqrt{r}\sqrt{d} = Dr^{3/2}$. Thus

$$\mathbb{E}_k \|\bar{G}_k^\varphi - M_k^\varphi\|_* \leq Dr^{3/2} \sqrt{\frac{v}{N}}.$$

This step uses independence across the sample index; it does not require independence across matrix entries.

Now consider the deterministic conditional bias. By the relative-bias assumption (this follows from Lemma E.4 and Lemma E.8 for $C_\tau(x)$ and $S_c(x)$),

$$\|M_k^\varphi - G_k\|_F \leq \rho \|G_k\|_F.$$

Therefore

$$\|M_k^\varphi - G_k\|_* \leq \sqrt{r} \|M_k^\varphi - G_k\|_F \leq \sqrt{r}\rho \|G_k\|_F \leq \sqrt{r}\rho \|G_k\|_*.$$

Combining the two bounds gives

$$\mathbb{E}_k \|\bar{G}_k^\varphi - G_k\|_* \leq Dr^{3/2} \sqrt{\frac{v}{N}} + \sqrt{r}\rho \|G_k\|_*. \quad (55)$$

Apply Lemma E.13 with $\bar{G}_k = \bar{G}_k^\varphi$, take conditional expectation, and use Equation (55):

$$\mathbb{E}_k F(X_{k+1}) \leq F(X_k) - \eta(1 - 2\sqrt{r}\rho) \|G_k\|_* + 2\eta Dr^{3/2} \sqrt{\frac{v}{N}} + \frac{L\eta^2 r}{2}.$$

Summing over $k = 0, \dots, T-1$, using $F(X_T) \geq \inf_X F(X)$, and dividing by ηT yields

$$(1 - 2\sqrt{r}\rho) A_T \leq \frac{\Delta}{\eta T} + \frac{L\eta r}{2} + 2Dr^{3/2} \sqrt{\frac{v}{N}},$$

where

$$A_T := \frac{1}{T} \sum_{k=0}^{T-1} \mathbb{E} \|G_k\|_*.$$

The choice $\eta = \sqrt{2\Delta/(LrT)}$ balances the first two deterministic terms and gives

$$\frac{\Delta}{\eta T} + \frac{L\eta r}{2} = \sqrt{\frac{2Lr\Delta}{T}}.$$

Dividing by $1 - 2\sqrt{r}\rho$ proves the lemma. \square

Theorem 5.6 (Pre-clipped Muon with hard clipping). *Under Assumptions 5.1 to 5.3, choose τ such that $\tau \geq B + \max\left\{\sigma\sqrt{2\log(16\sqrt{r})}, \frac{16\alpha\gamma\sqrt{r}}{\pi}\right\}$, and define $v_\tau := (1 - \alpha)\sigma^2 + \frac{4\alpha\gamma\tau}{\pi}$. Executing the update rule Equation (17) with $\varphi = C_\tau$ and a step size of $\eta = \sqrt{2\Delta/(LrT)}$ for T iterations yields:*

$$\frac{1}{T} \sum_{k=0}^{T-1} \mathbb{E}\|G_k\|_* \leq 2\sqrt{\frac{2Lr\Delta}{T}} + 4Dr^{3/2}\sqrt{\frac{v_\tau}{N}}. \quad (18)$$

Consequently, for $T \geq 32Lr\Delta/\varepsilon^2$ and $N \geq 64D^2r^3v_\tau/\varepsilon^2$, we guarantee $\frac{1}{T} \sum_{k=0}^{T-1} \mathbb{E}\|G_k\|_* \leq \varepsilon$.

Proof. At any iteration k , for gradient noise ξ_k with $0 \leq \sigma_k \leq \sigma$ and $0 \leq \gamma_k \leq \gamma$, hard clipping satisfies the relative-bias bound of Lemma E.4 and the variance bound of Lemma E.5. By Lemma E.11, the threshold assumed in the theorem gives $\rho_\tau \leq 1/(4\sqrt{r})$, so $1 - 2\sqrt{r}\rho_\tau \geq 1/2$. Applying Lemma E.14 with $v = v_\tau$ gives

$$\frac{1}{T} \sum_{k=0}^{T-1} \mathbb{E}\|G_k\|_* \leq 2\sqrt{\frac{2Lr\Delta}{T}} + 4Dr^{3/2}\sqrt{\frac{v_\tau}{N}},$$

which is the displayed theorem bound. The lower bounds on T and N make the two terms at most $\varepsilon/2$ each. \square

Theorem 5.7 (Pre-clipped Muon with smooth shrinkage). *Under Assumptions 5.1 to 5.3, choose $c \geq \max\left\{8\sqrt{r}\left[B + \sqrt{\frac{8}{\pi}}(1 - \alpha)\sigma\right], \frac{128\alpha\gamma\sqrt{r}}{\pi} \log\left(e + \frac{128\alpha\sqrt{r}}{\pi}\right)\right\}$, and define $v_c := (1 - \alpha)\sigma^2 + \frac{8\alpha\gamma c}{\pi e}$. Executing the update rule Equation (17) with $\varphi = S_c$ and a step size of $\eta = \sqrt{2\Delta/(LrT)}$ for T iterations yields:*

$$\frac{1}{T} \sum_{k=0}^{T-1} \mathbb{E}\|G_k\|_* \leq 2\sqrt{\frac{2Lr\Delta}{T}} + 4Dr^{3/2}\sqrt{\frac{v_c}{N}}. \quad (19)$$

Consequently, for $T \geq 32Lr\Delta/\varepsilon^2$ and $N \geq 64D^2r^3v_c/\varepsilon^2$, we guarantee $\frac{1}{T} \sum_{k=0}^{T-1} \mathbb{E}\|G_k\|_* \leq \varepsilon$.

Proof. At any iteration k , for gradient noise ξ_k with $0 \leq \sigma_k \leq \sigma$ and $0 \leq \gamma_k \leq \gamma$, Smooth shrinkage satisfies the relative-bias bound of Lemma E.8 and the variance bound of Lemma E.9. By Lemma E.11, the threshold assumed in the theorem gives $\rho_c \leq 1/(4\sqrt{r})$, so $1 - 2\sqrt{r}\rho_c \geq 1/2$. Applying Lemma E.14 with $v = v_c$ gives the displayed theorem bound. The lower bounds on T and N make the two terms at most $\varepsilon/2$ each. \square

F Experiment Details for Section 6

F.1 Gaussian Random Feature Regression

Hardware. The experiment was conducted on a CPU machine with AMD EPYC 7532 32-Core Processors.

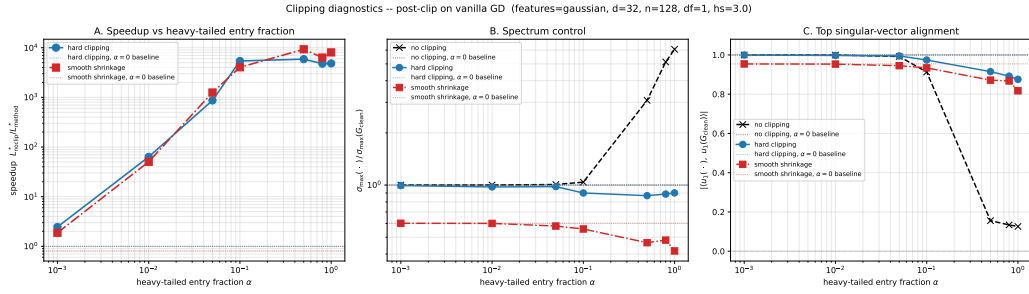
Problem setup. We minimize $L(W) = \frac{1}{2n} \|WA - Y\|_F^2$ where $W \in \mathbb{R}^{d_{\text{out}} \times d_h}$ and $A \in \mathbb{R}^{d_h \times n}$, feature matrix A follows i.i.d. standard Gaussian, and $Y = W^\sharp A$ with $W^\sharp \in \mathbb{R}^{d_{\text{out}} \times d_h}$ also i.i.d. standard Gaussian. We use $d_{\text{out}} = d_h = 32$, $n = 128$ and $d_{\text{out}} = d_h = 64$, $n = 256$ two settings.

Noise model. At each step, the true gradient $\nabla L(W_k) = \frac{1}{n} (W_k A - Y) A^T$ is corrupted by noise E_k drawn from the contamination model of Definition 3.2 with heavy-tailed component $H = t_1$ (Cauchy noise). We write $\tilde{G}_k := \nabla L(W_k) + E_k$ for the observed gradient. The contamination fraction α is selected over $\{0, 10^{-3}, 10^{-2}, 5 \times 10^{-2}, 10^{-1}, 0.5, 0.8, 1.0\}$. Each configuration is repeated over 10 random seeds (independent draws of A , W^\sharp , and noise E). We report the median loss curve.

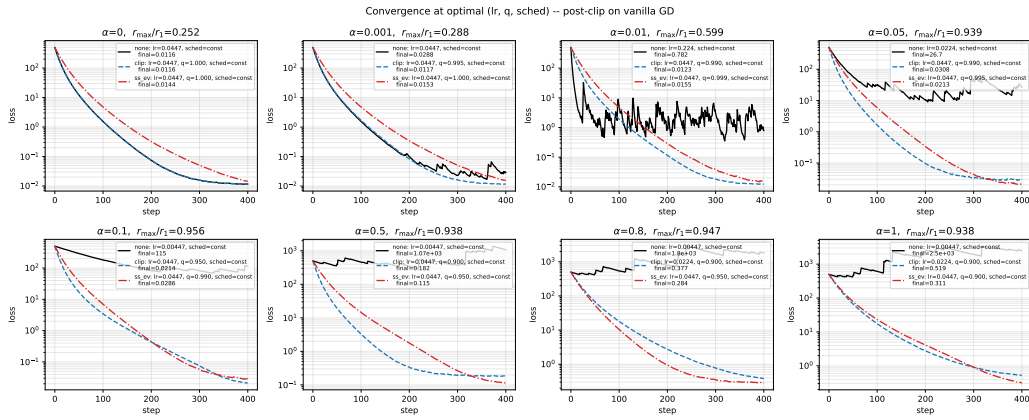
Methods. We compare six methods: vanilla GD and spectral GD (with spectral normalization implemented by SVD), each combined with one of three clipping maps. The clipping is applied at a different stage depending on the method: for vanilla GD, the map acts directly on the noisy gradient (*post-clipping*). For spectral GD, it acts on the noisy gradient before spectral normalization (*pre-clipping*). The three clipping maps are: (a) no clipping, (b) entry-wise hard clipping at threshold $C_\tau(x)$, and (c) smooth shrinkage $S_c(x)$. For (b) and (c), τ is set to the q -th quantile of $\{|\tilde{G}_{k,ij}|\}_{i,j}$ at each step, with $q \in \{0.90, 0.95, 0.99, 0.995, 0.999, 0.9995, 0.99999\}$. For each method we sweep the joint grid of learning rate $\eta \in \{0.001, 0.005, 0.01, 0.02, 0.05, 0.1\}$ and clipping quantile, and report the best final loss.

Results. *Post-clipping.* Results are shown in Figure 6 ($d = 32$) and Figure 7 ($d = 64$). Vanilla GD fails to converge once $\alpha \geq 10^{-2}$, whereas both clipping methods converge across all contamination strengths. In both dimensions, smooth shrinkage outperforms hard clipping when heavy-tailed noise dominates ($\alpha \geq 0.5$). Both methods also control the spectrum and help recovery of the rotated subspace (panel (a) of Figures 6 and 7).

Pre-clipping. Results are shown in Figure 8 ($d = 32$) and Figure 9 ($d = 64$). Spectral GD converges across all contamination strengths with or without pre-clipping; however, both hard clipping and smooth shrinkage *accelerate* spectral GD relative to the unclipped baseline beginning at $\alpha = 10^{-2}$, with the speedup growing as α increases. As in the post-clipping case, smooth shrinkage outperforms hard clipping for $\alpha \geq 0.5$. We observe similar spectral control and subspace recovery in both $d = 32$ and $d = 64$.

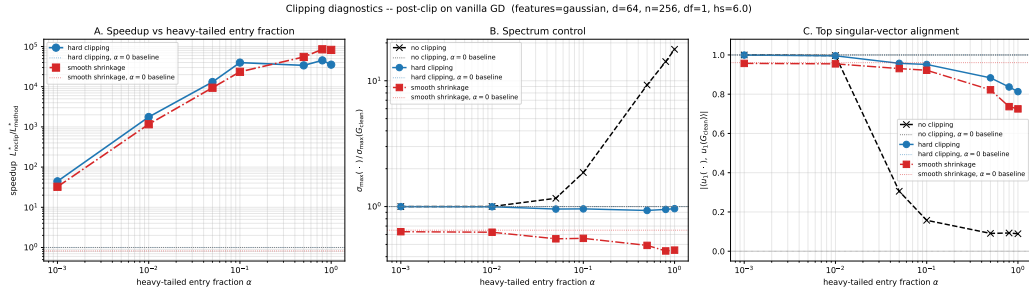


(a) Summary of speedup, spectral control, and subspace recovery across clipping methods and contamination strengths.

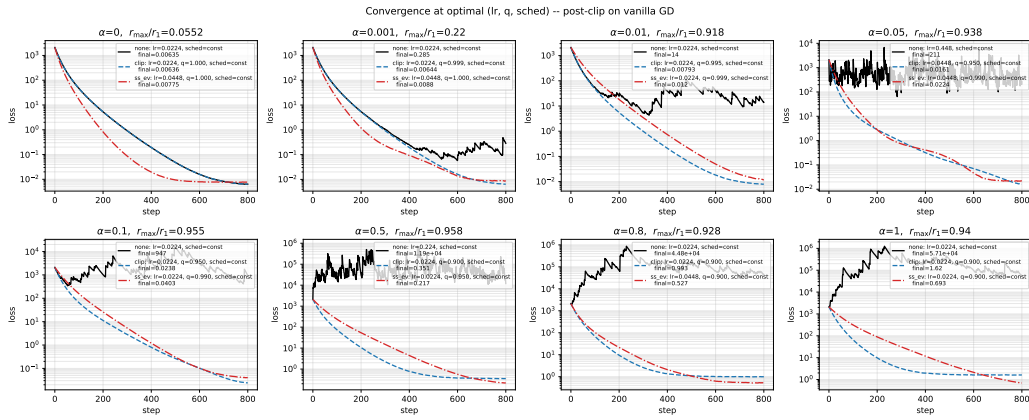


(b) Convergence under different clipping methods and contamination strengths.

Figure 6: Post Clipping for SGD under Gaussian random feature models ($d = 32$)

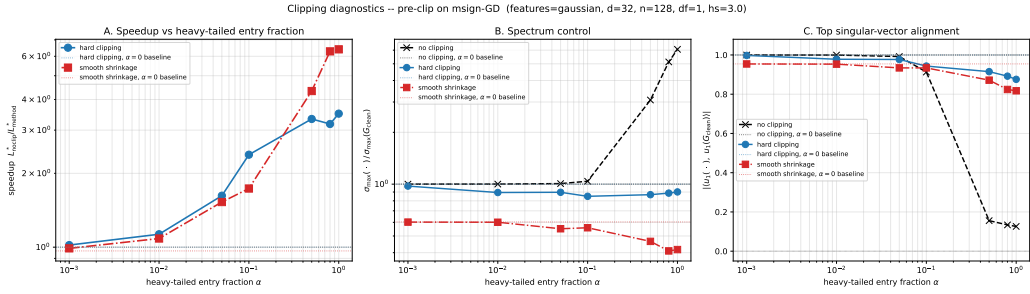


(a) Summary of speedup, spectral control, and subspace recovery across clipping methods and contamination strengths.

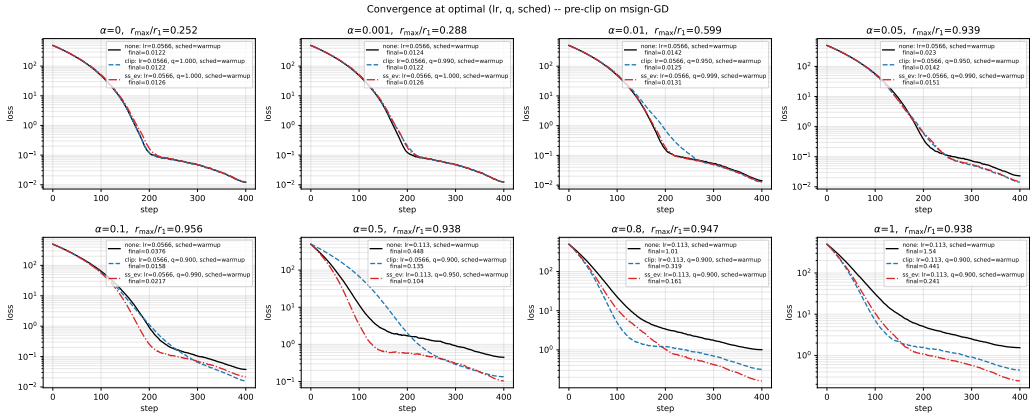


(b) Convergence under different clipping methods and contamination strengths.

Figure 7: Post Clipping for SGD under Gaussian random feature models ($d = 64$)

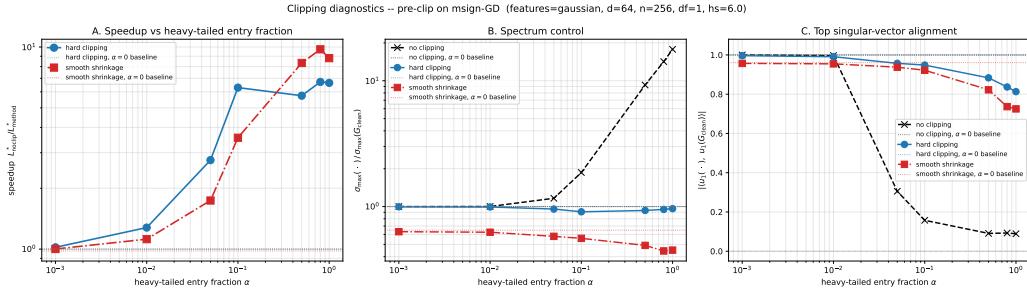


(a) Summary of speedup, spectral control, and subspace recovery across clipping methods and contamination strengths.

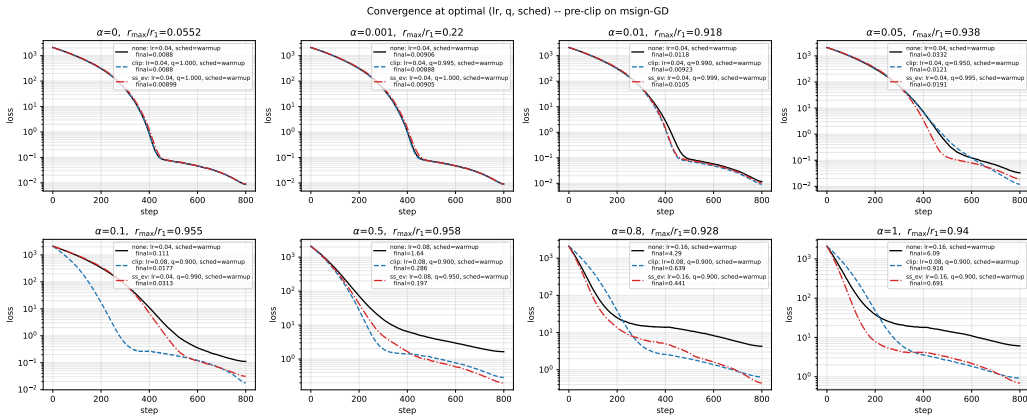


(b) Convergence under different clipping methods and contamination strengths.

Figure 8: Pre Clipping for spectral GD under Gaussian random feature models ($d = 32$)



(a) Summary of speedup, spectral control, and subspace recovery across clipping methods and contamination strengths.



(b) Convergence under different clipping methods and contamination strengths.

Figure 9: Pre Clipping for spectral GD under Gaussian random feature models ($d = 64$)

F.2 Language Model Pretraining

Hardware. The experiment was conducted on a single NVIDIA A100 GPU machine.

Model and data. We use the May 27, 2025 snapshot of modded-nanogpt [29] as the basis for our 276M-parameter NanoGPT experiments. This snapshot incorporates several modern architectural enhancements: rotary position embeddings, RMSNorm, a linear-decay learning-rate schedule, and squared-ReLU (ReLU^2) activations. It also features an untied output head, three additional value-embedding layers whose lookups are added to the attention values in the early transformer blocks, and a residual-stream U-net that connects early and late blocks via learned skip connections. Each embedding-style block contains approximately 38M parameters ($768 \times 50,257$); these four blocks—the untied output head together with the three value-embedding layers—account for 152M parameters, which combined with the 124M-parameter 12-layer transformer backbone yields a total of 276M parameters. We train on the 10B-token subset of FineWeb [30].

Methods. To test the effect of *post-clipping*, we apply two clipping maps φ , smooth shrinkage and hard clipping, to the AdamW [46] update $U_k = M_k / (\sqrt{V_k} + \varepsilon)$, i.e., $W_{k+1} = W_k - \eta \varphi(U_k)$. We compare them against unclipped AdamW. To test the effect of *pre-clipping*, we apply φ to the Nesterov momentum M_k before the matrix-sign step, i.e., $W_{k+1} = W_k - \eta \text{msign}(\varphi(M_k))$, where msign is computed via the Newton–Schulz iteration of Jordan et al. [1] and the update is rescaled by $0.2\sqrt{\max(n, m)}$ following Team et al. [5]. We compare these pre-clipping methods against Muon [1] and SPECTRA [14], with the latter applying spectral clipping to the Adam update via Newton–Schulz iterations.

Hyperparameters. We perform a grid search over learning rate \times clipping threshold for all clipping methods, where the clipping threshold is the q -th quantile of $|U_k|$ (post-clipping) or $|M_k|$ (pre-clipping). The unclipped baselines AdamW and Muon are swept over the same learning-rate grid; SPECTRA additionally decays its clipping threshold alongside the learning rate following a WSD [47] schedule. We sweep the learning rate over $\{1 \times 10^{-4}, 2 \times 10^{-4}, 6 \times 10^{-4}, 1 \times 10^{-3}, 1.6 \times 10^{-3}, 4 \times 10^{-3}\}$. The result of the learning-rate sweep is reported in Figure 10, and the best hyperparameter settings are listed in Table 3 and Table 4 for post- and pre-clipping, respectively.

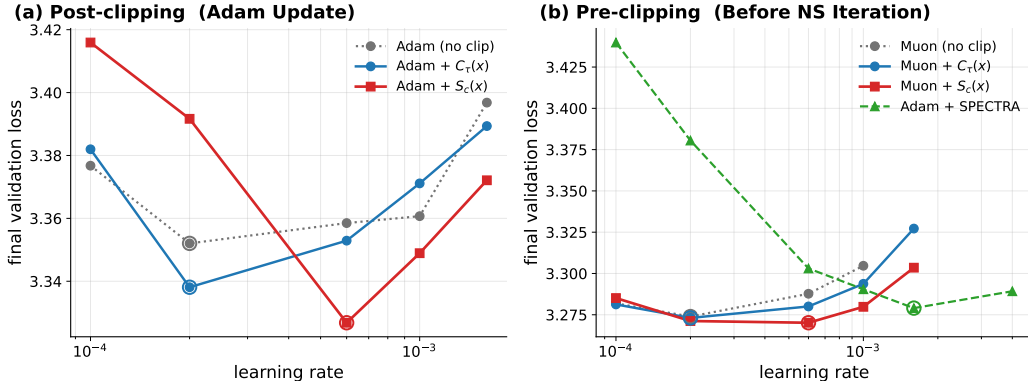


Figure 10: Learning-rate sweeps for post- and pre-clipping methods in terms of the final validation loss on NanoGPT.

Noise structure analysis. We investigate the structure of stochastic gradient noise. Let $G \in \mathbb{R}^{m \times n}$ denote the true gradient signal, approximated by averaging per-sample gradients over a large batch of 1024 sequences with 4096 tokens each. Let $U_G \in \mathbb{R}^{m \times r}$ and $V_G \in \mathbb{R}^{n \times r}$ collect the top- r left and right singular vectors of G , defining its signal subspace. Let g denote a single-sample stochastic gradient and the noise to be $E := g - G$.

Our goal is to measure how much the top entry of the noise matrix E perturbs the spectrum of G at different training stages (Theorem 3.3). We summarize this through the localization ratio $\hat{R}(E)$ in Definition 3.4. We report measurements of stochastic noise at

Table 3: Hyperparameter configurations for the optimizers evaluated for *post clipping* in Figure 4. β_1 and β_2 for AdamW are set to 0.9 and 0.99 by convention.

Hyperparameter	AdamW	AdamW $C_\tau(x)$	with AdamW $S_c(x)$	with
Learning Rate (η)	0.0002	0.0002	0.0006	
Clipping Quantile q	–	99.9%	99.5%	
Weight Decay	0.1	0.1	0.1	
Batch Size (tokens)	49152	49152	49152	
β_1 (First Moment)	0.9	0.9	0.9	
β_2 (Second Moment)	0.99	0.99	0.99	
ε (Stability)	10^{-8}	10^{-8}	10^{-8}	

Table 4: Hyperparameter configurations for the optimizers evaluated for *pre clipping* in Figure 4. β_1 for Muon is set to 0.95 by convention, SPECTRA uses Adam’s $\beta_1 = 0.9$.

Hyperparameter	Muon	SPECTRA	Muon $(C_\tau(x))$	Muon $(S_c(x))$
Learning Rate (η)	0.0002	0.0016	0.0002	0.0006
Clipping Quantile q	–	–	99.5%	99%
Weight Decay	0.1	0.1	0.1	0.1
Batch Size (tokens)	49152	49152	49152	49152
β_1 (First Moment)	0.95	0.9	0.95	0.95
β_2 (Second Moment)	–	0.99	–	–
ε (Stability)	–	10^{-8}	–	–

three training stages in Figure 11. Early in training (step 1000), nearly all layers’ stochastic noise has $\hat{R}(E) \ll 1$, indicating that the noise is aligned with the signal subspace. As training progresses, $\hat{R}(E)$ generally rises and exceeds 1, with the effect strengthening as k grows: the spike-like structure of E becomes increasingly pronounced when (u_k, v_k) are taken from subleading singular directions of G .

We further report the correlation between the top singular value and the largest entry of the stochastic gradient in Figure 12, and the Hill tail-index estimator across layers in Figure 13.



Figure 11: Localization ratio $\hat{R}(E_{\text{real}})$ of real stochastic noise plotted across layers at three training stages. Each row corresponds to a different singular direction of the signal G , from the leading direction (top row) to the 8th (bottom). The thick dashed line at $y = 1$ marks the Gaussian null baseline, at which the noise is delocalized and matches the random-matrix prediction. As training progresses, $\hat{R}(E)$ generally rises and exceeds 1, with the effect strengthening as k grows.

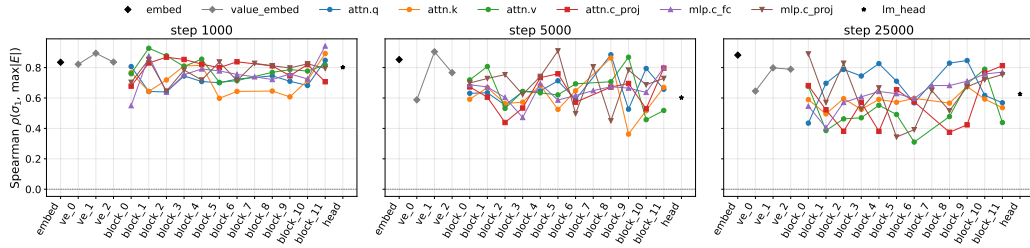


Figure 12: Correlation between the top singular value and the largest entry of the stochastic noise.

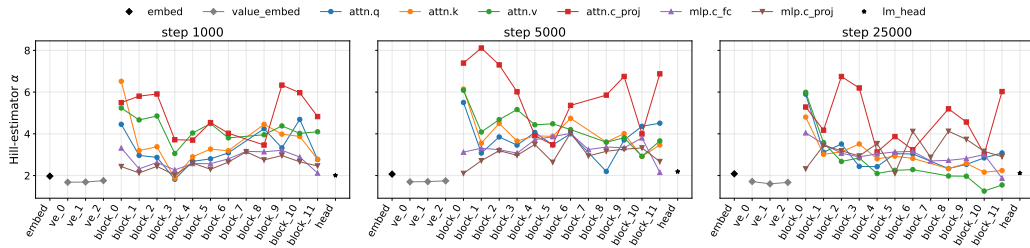


Figure 13: Hill tail-index estimator for stochastic noise across different layers at different stages. Layers will become more heavy-tailed as the training progresses.